DMD Fast Forward. Published on April 2, 2010 as DOI: 10.1124/dmd.110.032755
DMD Fast Forward. Published on April 2, 2010 as doi:10.1124/dmd.110.032755
This article has not been copyedited and formatted. The final version may differ from this version.

DMD #32755

Metabolism and Disposition of [^{14}C]BMS-690514 ((3R,4R)-4-amino-1-((4-((3-methoxyphenyl)amino)pyrrolo[2,1-f][1,2,4]triazin-5-yl)methyl)-3-piperidinol) Following Oral Administration to Rats, Rabbits and Dogs

Haizheng Hong, Hong Su, Haojun Sun, Alban Allentoff, Ihoezo V. Ekhato, Theodore Chando, Janet Caceres-Cortes, Vikram Roongta, Ramaswamy A. Iyer, W. Griffith Humphreys, and Lisa J. Christopher

AFFILIATIONS:

Departments of Pharmaceutical Candidate Optimization (H.H., H.Su., T.C., J. C-C., V.R., R.A.I., W.G.H. and L.J.C.) and Radiochemistry (H. Sun., A.A. and I.V.E.)

Bristol-Myers Squibb Pharmaceutical Research and Development, Princeton, New Jersey

Downloaded from dmd.aspetjournals.org at ASPET Journals on April 18, 2024

Copyright 2010 by the American Society for Pharmacology and Experimental Therapeutics.

DMD Fast Forward. Published on April 2, 2010 as DOI: 10.1124/dmd.110.032755
This article has not been copyedited and formatted. The final version may differ from this version.

Running Title: Disposition of BMS-690514 in Rats, Dogs and Rabbits

ADDRESS CORRESPONDENCE TO:

Haizheng Hong, Ph.D.

Department of Biotransformation

Bristol-Myers Squibb Research & Development

Route 206 & Province Line Road

Mail Stop F13-09

Princeton, NJ 08543

Tel: 609-252-5769

Fax: 609-252-6802

E-mail: haizheng.hong@bms.com

NUMBER OF TEXT PAGES: 44

NUMBER OF TABLES: 4

NUMBER OF FIGURES: 7

NUMBER OF REFERENCES: 29

NUMBER OF WORDS IN ABSTRACT: 249 words

NUMBER OF WORDS IN INTRODUCTION: 614 words

NUMBER OF WORDS IN DISCUSSION: 1493 words

ABBREVIATIONS:

AUC, area under the curve; BDC, bile duct-cannulated; HPLC, high-performance liquid chromatography; LC/MS/MS, liquid chromatography/tandem mass spectrometry; LSC, liquid scintillation counting.

Downloaded from dmd.aspetjournals.org at ASPET Journals on April 18, 2024

DMD Fast Forward. Published on April 2, 2010 as DOI: 10.1124/dmd.110.032755
This article has not been copyedited and formatted. The final version may differ from this version.

Abstract

BMS-690514 is a potent inhibitor of human epidermal growth factor receptor (HER)1, 2, and 4 and vascular endothelial growth factor receptor (VEGFR) 1-3. BMS-690514 is an oral oncologic agent currently being developed for the treatment of patients with advanced NSCLC and breast cancer. In this investigation, a series of studies were conducted to determine the biotransformation of [^{14}C]BMS-690514 following oral administration to rats, rabbits and dogs. After administration of a single oral dose of [^{14}C]BMS-690514 to rats and dogs, the majority of the radioactive dose (61-71%) was recovered in the feces, while 18-20% was eliminated in urine. In bile duct-cannulated (BDC) rats, 83 and 17% of the administered radioactivity was recovered in the bile and urine, respectively, suggesting that biliary secretion was a major route for the elimination of BMS-690514-derived radioactivity in rats. The parent compound underwent extensive metabolism in both species, with <12% of the administered radioactivity recovered as BMS-690514 in the excreta samples. Metabolite profiles in plasma were qualitatively similar in rats, rabbits and dogs. Unchanged BMS-690514 was a prominent drug-related component in the plasma profiles from all species. However, multiple metabolites contributed significantly to the circulating radioactivity, particularly for rabbit and dog, where metabolites comprised 73-93% of the area under the time curve (0-8 h). Circulating metabolites included M6, a direct *O*-glucuronide conjugate, M1, a hydroxylated metabolite, and glucuronide conjugates of hydroxylated and *O*-demethylated metabolites. Overall, the results from these studies suggested that BMS-690514 was well-absorbed and highly metabolized through multiple pathways in these preclinical species.

Downloaded from dmd.aspetjournals.org at ASPET Journals on April 18, 2024

DMD Fast Forward. Published on April 2, 2010 as DOI: 10.1124/dmd.110.032755
This article has not been copyedited and formatted. The final version may differ from this version.

Introduction

The human epidermal growth factor receptor (HER, including EGFR) and vascular endothelial growth factor receptor (VEGFR) signaling pathways are key components in cancer pathogenesis and progression (Herbst et al., 2005; Tortora et al., 2008). While multiple agents targeting these individual pathways have demonstrated utility in treating advanced non-small cell lung cancer (NSCLC) and other solid tumors (Fukuoka et al., 2003; Kris et al., 2003; Shepherd et al., 2005; Sandler et al., 2006; Reck et al., 2009), recent literature has suggested the potential for enhanced antitumor efficacy through the simultaneous inhibition of both EGFR and VEGFR pathways (Tabernero, 2007; Tortora et al., 2008).

BMS-690514 ((3R,4R)-4-amino-1-((4-((3-methoxyphenyl)amino)pyrrolo[2,1-f][1,2,4]triazin-5-yl)methyl)-3-piperidinol) is a highly selective and potent inhibitor of multiple receptors in the HER and VEGFR families, including EGFR, HER2 and HER4 and VEGFR 1-3. It is currently under clinical development as an oral treatment for NSCLC, metastatic breast cancer and other solid malignancies (Bahleda et al., 2008; Bahleda et al., 2009). Preclinical studies have shown that BMS-690514 exerts its antiproliferative and proapoptotic effects on NSCLC cell lines expressing activating mutations such as exon19 del and L858R as well as deactivating mutations such as T790M, known to impart resistance to other EGFR tyrosine kinase inhibitors (de La Motte Rouge et al., 2007) and in human xenograft models dependent upon EGFR and HER2 signaling (Wong et al., 2007).

Downloaded from dmd.aspetjournals.org at ASPET Journals on April 18, 2024

DMD Fast Forward. Published on April 2, 2010 as DOI: 10.1124/dmd.110.032755
This article has not been copyedited and formatted. The final version may differ from this version.

The pharmacokinetic properties of BMS-690514 in pre-clinical species supported an oral clinical development program in patients with solid tumors (Marathe et al., 2010). BMS-690514 was well-absorbed in mouse, rat and dog, with mean bioavailabilities ranging from 29.4% in dogs to nearly 100% in rats; the mean bioavailability in monkey was only 8.1%, possibly due to high first-pass metabolism. The volume of distribution ranged from 1.9 to 8.7 L/kg in these animal species, indicating distribution outside of the vascular compartment. In incubations with hepatocytes from animals and humans, BMS-690514 was metabolized to several oxidative metabolites, including hydroxylated metabolites and an *O*-demethylated metabolite. In addition, a direct glucuronide conjugate was formed in most animal species and was a prominent metabolite in human hepatocytes (Marathe et al., 2010).

In vivo disposition and metabolism information is critical in all phases of a fully integrated drug development program, and these studies are typically performed with either C-14 or tritium-labeled material to provide detailed quantitative information on the parent drug and its metabolites. In the current studies, the comparative metabolism of BMS-690514 was assessed in rats, rabbits and dogs after oral administration of [^{14}C]BMS-690514. Comprehensive mass-balance and metabolite profiling of plasma and excreta samples was performed for rat and dog, the primary species utilized for toxicological evaluation of the compound. In addition, plasma metabolite profiles were obtained from rabbit, a supplemental species utilized in reproductive toxicology studies. Metabolite profiles from these studies were retained for comparison to clinical samples. Metabolites of BMS-690514 were identified by liquid chromatography with tandem mass

Downloaded from dmd.aspetjournals.org at ASPET Journals on April 18, 2024

DMD Fast Forward. Published on April 2, 2010 as DOI: 10.1124/dmd.110.032755
This article has not been copyedited and formatted. The final version may differ from this version.

spectrometry (LC/MS/MS). Selected metabolites were isolated and further characterized by nuclear magnetic resonance (NMR).

A previous study with bile duct-cannulated (BDC) rats using non-radiolabeled BMS-690514 showed that the parent drug and metabolites were excreted via biliary and renal routes (Marathe et al., 2010), with glucuronide conjugates mainly excreted in the bile. It has been known that glucuronides typically undergo hydrolysis in the gastrointestinal (GI) tract by gut flora before excretion in the feces (Parker et al., 1980; Christopher et al., 2008). Therefore, the current studies included administration of [^{14}C]BMS-690514 to BDC rats to understand its overall disposition, particularly for conjugated metabolites excreted in the bile.

Based on these *in vivo* animal metabolism and disposition data as well as the results from earlier *in vitro* studies (Marathe et al., 2010), potential human *in vivo* biotransformation pathways of BMS-690514 were proposed.

Downloaded from dmd.aspetjournals.org at ASPET Journals on April 18, 2024

DMD Fast Forward. Published on April 2, 2010 as DOI: 10.1124/dmd.110.032755
This article has not been copyedited and formatted. The final version may differ from this version.

Materials and Methods

Chemicals. [^{14}C]BMS-690514 with a specific activity of 36.8 μCi/mg and radiochemical purity of 98.96% was supplied by the Radiochemistry Group of the Department of Chemical Synthesis, Bristol Myers-Squibb (BMS), Princeton, NJ, USA. The C-14 label was evenly distributed among the six carbons of the methoxyaniline ring as indicated in Figure 1. Non-radiolabeled BMS-690514 and reference standards for M2, the 3-methoxy, 4-hydroxy aniline metabolite and M6, an ether glucuronide of BMS-690514, were also supplied by BMS Research & Development.

All chemical reagents were purchased from Sigma-Aldrich Chemical Co. (St. Louis, MO) except where indicated. Solvents used for high-performance liquid chromatography (HPLC) analysis were of HPLC grade. Ecolite™ liquid scintillation cocktail was purchased from MP Biomedicals, Inc. (Irvine, CA). Permafluor E+ and Emulsifier-Safe scintillation cocktails were obtained from PerkinElmer, Inc. (Waltham, MA)

Dosing of Animals and Collection of Samples. All the animal studies were conducted after approval of protocols by the Institutional Animal Care and Use Committee in approved facilities. For each study, a dosing solution was prepared by dissolving appropriate amounts of radiolabeled and non-radiolabeled BMS-690514 in dilute hydrochloric acid (0.01 to 0.02 N) to achieve the desired specific activity.

Intact Rat Study. Twenty-one fasted male Sprague-Dawley rats (Charles River, Wilmington MA), weighing approximately 290-320 g, were each administered an oral solution dose of [^{14}C]BMS-690514 at a target dose of 15 mg/kg (100 μCi/kg). The animals were fasted prior to dosing. The dose solutions were administered by oral gavage

Downloaded from dmd.aspetjournals.org at ASPET Journals on April 18, 2024

DMD Fast Forward. Published on April 2, 2010 as DOI: 10.1124/dmd.110.032755
This article has not been copyedited and formatted. The final version may differ from this version.

in a volume of 5 ml/kg. Terminal blood samples were collected from one group of animals (n = 3 animals per time point) at 1, 2, 4, 8, and 24 hours after dosing and blood samples were centrifuged to obtain plasma for biotransformation analyses. Another group of 3 animals were individually housed in metabolism cages for the separate collection of urine and feces. Urine was collected at 0-12, 12-24, and in 24-h intervals up to 168 h. Upon collection, urine samples were acidified with concentrated formic acid, such that the final acid concentration was 1% (v/v). Feces were collected in 24-h intervals from 0-168 h. The fecal samples were homogenized with four volumes of 20% ethanol in water. Cage rinses were performed after each collection interval, and a cage wash was performed at the end of the study period. Excreta and cage residue samples were analyzed for total radioactivity. A third group of animals were received from the supplier instrumented with jugular vein catheters for serial blood collection. Blood samples (0.25 ml per time point) were collected before dosing and at 0.5, 1, 2, 4, 8, 12 and 24 h after dosing for determining the pharmacokinetics of total radioactivity in plasma.

BDC Rat Study. Three bile-duct cannulated (BDC) Sprague-Dawley rats, weighing 262-283 g, were each administered an oral dose of [^{14}C]BMS-690514 at a target level of 15 mg/kg (100 μCi/kg). The animals were fasted prior to the dosing and the dose solutions were administered by oral gavage in a volume of 5 ml/kg. Blood samples, 1 mL each, were collected from each rat at 1 h and 4 h post-dose and terminal blood samples were collected from each animal at 24 h for confirmation of exposure. Urine and bile samples for biotransformation profiling were collected over the intervals of 0-8 h and 8-24 h post-dose. Upon collection, urine samples were acidified with formic acid to a final concentration of 1% (v/v). The fecal samples were collected over the 0-24 h time interval

Downloaded from dmd.aspetjournals.org at ASPET Journals on April 18, 2024

DMD Fast Forward. Published on April 2, 2010 as DOI: 10.1124/dmd.110.032755
This article has not been copyedited and formatted. The final version may differ from this version.

and homogenized with three volumes of 20% methanol in water.

Intact Rabbit Study. Three female New Zealand White rabbits, weighing approximately 3.5-4.0 kg, were each administered an oral dose of [^{14}C]BMS-690514 at a target dose level of 5 mg/kg (30 μCi/kg). The animals were fasted overnight prior to dosing, and doses were administered by oral gavage in a dose volume of 2 ml/kg. Blood samples (5 ml per time point) were collected from each animal predose and at 1, 2, 4, 8 and 24 h after dosing for identification of metabolites in plasma.

Intact Dog Study. Three male beagle dogs, weighing approximately 8.5-10.7 kg, were each administered a single oral dose of [^{14}C]BMS-690514 at a target dose of 10 mg/kg (20 μCi/kg). The animals were fasted prior to dosing. The doses were administered by oral gavage in a volume of 2 ml/kg. Blood samples (2 ml per time point) were collected from each animal predose and at 0.5, 1, 2, 4, 8, 12 and 24 h after dosing for determining the pharmacokinetics of in plasma. Additional blood samples for biotransformation analysis were collected from each animal predose and at 1, 2, 4, 8, and 24 h after dosing. All blood samples were centrifuged to obtain plasma. Urine was collected from 0-12 h, 12-24 h, and in 24 h intervals thereafter, up to 168 h; the samples were acidified with formic acid to a final concentration of 1% (v/v). Feces were collected from 0-168 h in 24 h intervals. The fecal samples were homogenized with four volumes of 20% ethanol in water. Cage debris was collected after each daily post-dose excreta collection; and a cage wash was performed at the end of the study period. Excreta and cage residue samples were analyzed for total radioactivity.

Downloaded from dmd.aspetjournals.org at ASPET Journals on April 18, 2024

DMD Fast Forward. Published on April 2, 2010 as DOI: 10.1124/dmd.110.032755
This article has not been copyedited and formatted. The final version may differ from this version.

Analysis of Radioactivity. Portions of plasma, bile and urine (50-100 µl) and cage wash/rinse samples (300 µl volumes) were added to 5 to 15 ml of Ecolite^{TM} or Emulsifier-Safe scintillation mixture and analyzed directly by liquid scintillation counting. Portions of fecal homogenate from the BDC rat study (approximately 0.2 g each) were incubated overnight at 60°C with Soluene-350 to solubilize the samples. After cooling, 0.2 ml of 30% hydrogen peroxide was added to each sample. The samples were mixed with scintillation mixture (Ecolite^{TM}) and counted on a Packard Tricarb 3200CA liquid scintillation counter (PerkinElmer Inc., Boston, MA). In other studies, aliquots of fecal homogenates, 0.2 to 0.5 g, were air-dried and combusted with a model 307 or model 387 Sample Oxidizer (PerkinElmer Inc.). The liberated $^{14}CO_2$ was trapped into Carbo-Sorb E (PerkinElmer Inc.) mixed with Permafluor E scintillation fluid, and analyzed by LS6500 liquid scintillation counter (Beckman Instruments). The efficiency of the sample oxidizer was determined before combusting experimental samples. Three levels of radioactivity corresponding to low, medium, and high [^{14}C]standards were placed into cones and pads and combusted. The combusted standards were analyzed by liquid scintillation counting along with equivalent levels of the [^{14}C]standards spiked into scintillation fluid. The average disintegrations per minute in combusted samples were compared with the spiked samples to determine the combustion efficiency. Combustion efficiency for fecal samples was considered acceptable if the recovery of radioactivity was >90%. In all cases, scintillation data were corrected for counting efficiency using appropriately prepared quench curves. The radioactivity in plasma, urine, bile, and feces was reported as nanogram-equivalents of BMS-690514 per ml or per gram or as a percentage of the administered dose.

Downloaded from dmd.aspetjournals.org at ASPET Journals on April 18, 2024

DMD Fast Forward. Published on April 2, 2010 as DOI: 10.1124/dmd.110.032755
This article has not been copyedited and formatted. The final version may differ from this version.

Preparation of Biological Samples for Analysis. Representative pooled urine samples from intact rats (5% pool, 0-168 h), BDC rats (2% pool, 0-24 h), dogs (5% pool, 0-168 h) were prepared by combining a constant percentage of the volume excreted from each animal during each collection interval. Representative pooled fecal homogenate samples from intact rats (2% pool, 0-168 h) and dogs (2% pool, 0-168 h) were prepared by combining an approximately constant percentage of weight excreted from each animal during each collection interval. Representative pooled bile samples from BDC rats (2% pool, 0-24 h) were prepared by combining a constant percentage of the bile volume excreted from each animal during each collection interval. Plasma samples were segregated by collection time and equal volumes from each animal were combined.

Pooled plasma and fecal samples were extracted with methanol/acetonitrile (50:50 v/v) at a ratio of 3 volumes solvent per 1 volume of sample. The mixtures were vortex mixed, sonicated for 5 min, and centrifuged (Eppendorf Centrifuge 5810R, Hamburg, Germany) at 2500 g for 20 min. The resulting supernatants were transferred into new tubes and the precipitated pellets were extracted two additional times with 2 volumes of methanol:acetonitrile:water (25:25:50 v/v/v). The total extraction recovery for all samples ranged from 85 to 99%. The replicate extracts for a given sample were combined and evaporated to dryness under nitrogen in a TurboVap Evaporator (Zymark, Inc., Hopkinton, MA). The resulting residues were reconstituted in methanol:acetonitrile:water (25:25:50 v/v/v). Pooled urine and bile samples were centrifuged at 9000 g for 10 min prior to biotransformation profiling and mass spectrometic analysis.

Radiochromatographic Analysis of Metabolites. Biotransformation profiling was performed on a Surveyor high-performance liquid chromatography (HPLC) system

Downloaded from dmd.aspetjournals.org at ASPET Journals on April 18, 2024

DMD Fast Forward. Published on April 2, 2010 as DOI: 10.1124/dmd.110.032755
This article has not been copyedited and formatted. The final version may differ from this version.

equipped with an autosampler and photodiode-array detector (ThermoFisher, Waltham, MA). Sample components were separated on a Waters YMC ODS-AQ HPLC column (4.6 x 150 mm, 120 Å, 5 μm particle size) maintained at ambient temperature. The mobile phase consisted of two solvents: mobile phase A (95% water and 5% acetonitrile (v/v) containing 10 mM ammonium acetate, pH 5.0) and mobile phase B (100% acetonitrile). The linear gradient program used for HPLC separation was as follows: hold isocratic at 0% B (0–5 min); linear gradient from 0 to 28% B (5–50 min); linear gradient from 28 to 90% B (50–55 min); hold isocratic at 90% B (55–60 min). The mobile phase flow rate was 1.0 ml/min and the column eluate was monitored at a wavelength of 307 nm. An accurate post-column splitter (LC-Packings, San Francisco, CA) was installed after the PDA detector, diverting 25% of the eluate to a ThermoFisher LCQ Deca XP-Plus ion trap mass spectrometer and the remaining 75% of the eluate to a fraction collector (Gilson, Middleton, WI), where the flow was collected in 96-well Luma plates (PerkinElmer Life Sciences, Boston, MA) with a collection rate of 0.25 min/well. The plates were evaporated to dryness on a Savant Speed-Vac (Savant Instruments Inc., Holbrook, NY) and counted for radioactivity (10 min/well) with a TopCount® Microplate Scintillation Counter (PerkinElmer Life Sciences, Boston, MA).

The LCQ Deca XP-Plus mass spectrometer was equipped with an electrospray ionization source operated in positive-ion mode with a capillary temperature of 350°C and spray voltage of 5 kV. The nitrogen gas flow rate, capillary voltage and the tube lens voltages were periodically adjusted to give maximum sensitivity or fragmentation of drug-related components. Product ions were generated via collision-induced dissociation with helium using normalized collision energy of 30% and a precursor ion isolation width of *m/z* 2.0.

Downloaded from dmd.aspetjournals.org at ASPET Journals on April 18, 2024

DMD Fast Forward. Published on April 2, 2010 as DOI: 10.1124/dmd.110.032755
This article has not been copyedited and formatted. The final version may differ from this version.

For exact mass measurement, 25% of the column eluate was diverted to a LTQ Orbitrap Discovery (ThermoFisher), which was equipped with an electrospray ionization source operated in positive-ion mode. The capillary temperature was 350°C and the spray voltage was 4 kV. The resolving power for full-scan event and MS/MS spectrometric events were set at 30,000 and 15,000, respectively. Prior to analysis of study samples, the instrument was calibrated with a calibration solution; the instrument was deemed acceptable for use if the mass accuracy for all components in the calibration solution were within 5 ppm of their expected values.

Pharmacokinetic Analyses. For each species, the concentration of total drug-related radioactivity in plasma samples (ng-equivalents/ml) was determined from the mean radioactivity of n = 3 animals per time point and the administered specific activity. The concentration of parent compound was determined by multiplying the percent contribution of the BMS-690514 in the pooled radioprofile by the total radioactivity concentration for each time point. The area under the time curve AUC (0-8 h) values for total radioactivity and BMS-690514 were determined using Microsoft Excel with the trapezoidal method. The concentrations at the 1, 2, 4 and 8 h were used in the calculation of AUC (0-8 h) for total radioactivity and BMS-690514 in rats, rabbits and dogs.

Isolation of Metabolites M6, M7, M8 and M24. Metabolites M6, M7, M8 and M24 were isolated from rat bile collected after oral administration of [^{14}C]BMS-690514. Prior to HPLC separation, the pooled bile sample was concentrated on a Waters Sep-Pak® Vac 35 cc (10 g) C18 solid-phase extraction cartridge preconditioned with methanol, acetonitrile, water and then 50 µM ammonium acetate (pH 5). The bile sample (diluted

Downloaded from dmd.aspetjournals.org at ASPET Journals on April 18, 2024

DMD Fast Forward. Published on April 2, 2010 as DOI: 10.1124/dmd.110.032755
This article has not been copyedited and formatted. The final version may differ from this version.

approximately 5-fold in 50 µM ammonium acetate) was applied to the cartridge. After loading the sample, the cartridge was washed with water and metabolites were then eluted with acetonitrile/water (50:50, v/v). The acetonitrile /water eluate was evaporated to dryness and reconstituted in 10 mM ammonium acetate (pH 5).

M6, M7, M8 and M24 were isolated from the concentrated sample using a Waters 2695 HPLC equipped with a PDA detector and a YMC ODS-AQ 4.6 × 150 mm column (Waters Corp., Milford, MA). The mobile phase consisted of two solvents: mobile phase A (95% water and 5% acetonitrile (v/v) containing 10 mM ammonium acetate, pH 5.0) and mobile phase B (100% acetonitrile). The linear gradient program used for HPLC separation was as follows: hold isocratic at 0% B (0–5 min); linear gradient from 0 to 25% B (5–45 min); hold isocratic at 25% B (45-50 min); linear gradient from 25 to 90% B (50–55 min); hold isocratic at 90% B (55–60 min).

Treatment of M24 with *β*-glucuronidase. Isolated M24 was treated with *β*-glucuronidase at an enzyme concentration of 800 U/ml in 40 mM sodium acetate buffer (pH 5.1). The reaction was conducted at 37°C in a shaking water bath for 90 min. At the end of reaction, an equal volume of ice-cold acetonitrile was added to quench the reaction. The samples were vortex mixed and centrifuged at 13,000 rpm for 10 min and the supernatant was analyzed by LC-MS/MS on the LTQ-Orbitrap system described above.

NMR Analysis. BMS-690514 and isolated metabolites M6, M7 and M8 (about 200 µg each) were each dissolved in D_2O:acetonitrile-d_3 (50:50, v/v) and transferred to 3 mm NMR tubes. The samples were analyzed using Bruker Advance 600 and 700 MHz NMR

Downloaded from dmd.aspetjournals.org at ASPET Journals on April 18, 2024

DMD Fast Forward. Published on April 2, 2010 as DOI: 10.1124/dmd.110.032755
This article has not been copyedited and formatted. The final version may differ from this version.

spectrometers equipped with a 5-mm cryo triple resonance probe (Bruker, Billerica, MA) at 30 °C. All the ^{1}H chemical shifts were reported on the δ scale (ppm) downfield from tetramethylsilane. ^{13}C chemical shift data were deduced from heteronuclear multiple-bond correlation spectroscopy (HMBC). The peak assignment was based on ^{1}H, ^{1}H-^{1}H-gradient correlation spectroscopy and ^{1}H-^{13}C-HMBC spectroscopy analysis. ACD/NMR prediction software was obtained from Advanced Chemistry Development Inc. (Toronto, ON, Canada).

Downloaded from dmd.aspetjournals.org at ASPET Journals on April 18, 2024

DMD Fast Forward. Published on April 2, 2010 as DOI: 10.1124/dmd.110.032755
This article has not been copyedited and formatted. The final version may differ from this version.

Results

Excretion of the Radioactive Dose. The recovery of radioactivity in the urine and feces of intact rats and dogs and in urine, bile and feces from BDC-rats following administration of a single oral dose of [^{14}C]-BMS-690514 is summarized in Table 1. In intact rats and dogs, the majority of the radioactive dose was recovered in the feces. The fecal excretion of radioactivity in intact rats and dogs in the 0-168 h interval post-dose was 71.2% and 60.8% of the dose, respectively. For both species, a significant portion of radioactivity was also eliminated in the urine. Urinary excretion of the dose was 18.4% and 20.1% in intact rats and dogs, respectively. The total recovery of the radioactive dose in these two studies was >89%. After oral administration to BDC rats, 83.4% of the administered dose was recovered in the bile, 17.1% in the urine and 5.8% in the feces over the 24-h interval post-dose.

Plasma Concentration Profiles of Radioactivity and BMS-690514. The plasma concentration versus time pharmacokinetic profiles for total radioactivity and BMS-690514 after administration of single oral dose of [^{14}C]-BMS-690514 to intact rats, rabbits and dogs are shown in Figure 2A-C. For all the 3 species, the plasma concentration of total radioactivity was significantly higher than the plasma concentration of BMS-690514 at all time points up to 8 h. The AUC (0-8 h) values for BMS-690514 and total radioactivity were 5420 and 9456 ng-h/ml in rats, 709 and 10,167 ng-h/ml in rabbits and 3340 and 12,389 ng-h/ml in dogs, respectively. Based on these exposure data, BMS-690514 comprised approximately 57%, 7% and 27%, of the AUC (0-8 h) of total radioactivity in rats, rabbits and dogs, respectively (Figure 2).

Downloaded from dmd.aspetjournals.org at ASPET Journals on April 18, 2024

DMD Fast Forward. Published on April 2, 2010 as DOI: 10.1124/dmd.110.032755
This article has not been copyedited and formatted. The final version may differ from this version.

Metabolite Profiles in Plasma. Representative biotransformation profiles of BMS-690514 in plasma from rats, rabbits and dogs at 2 h post-dose are shown in Figure 3A-C, and the distribution of drug-related components in rat, rabbit and dog plasma is summarized in Table 2. Plasma biotransformation profiles were qualitatively similar between the species. Parent drug BMS-690514 (P), a direct glucuronide conjugate (M6), a hydroxylated re-arrangement product (M1), and glucuronide conjugates of oxidative metabolites (M7, M8 and M9) were prominent drug-related components in the plasma from rats, rabbits, and dogs.

Metabolite Profiles in Urine. Representative radio-profiles of pooled urine samples collected in the 0-168 h after oral administration of [^{14}C]-BMS-690514 to rats and dogs are shown in Figure 4A and 4D, respectively. The urinary biotransformation profiles were qualitatively similar in rats and dogs. In total, BMS-690514 and 10 drug-related products were identified in the urine profiles in these two species (Table 3). Unchanged parent drug (P), oxidative metabolites M2, M3 and M37 and glucuronide conjugates M6, M7, M8 and M9, were the prominent drug-related components in the urine from both species. Approximately 5.0 and 1.0% of the administered radioactivity was recovered as parent compound in the urine of rats and dogs, respectively. Several early-eluting peaks (eluting before 10 min) present in the profiles from the two species could not be identified due to high mass spectrometric interference. These early-eluting peaks accounted for 5.9 and 10.7% of the radioactivity in pooled rat and dog urine (0-168 h), respectively.

Metabolite Profiles in Feces. Representative radio-profiles of pooled fecal samples collected in the 0-168 h after oral administration of [^{14}C]-BMS-690514 to rats and dogs

Downloaded from dmd.aspetjournals.org at ASPET Journals on April 18, 2024

DMD Fast Forward. Published on April 2, 2010 as DOI: 10.1124/dmd.110.032755
This article has not been copyedited and formatted. The final version may differ from this version.

are shown in Figures 4B and 4E and the distribution of metabolites is shown in Table 3. BMS-690514 (P), and metabolites M2, M3 and M37 were prominent peaks in each of the fecal profiles. The parent compound accounted for 6.8 and 2.3% of the administered dose in the feces of rats and dogs, respectively. Metabolites M2 and M37 together accounted for 6.9 and 15.6% of the dose in rat and dog feces, respectively, while M3 accounted for <8.2 and 16.3% of the dose in these matrices. M6 accounted for 4.8% of the dose in fecal samples from dogs, but was not identified in the feces from rats. Other prominent biliary glucuronide-conjugated metabolites, M7, M8 and M9, were not detected in the fecal samples from either species.

An additional oxygenated metabolite, M26, was detected in the fecal profile from rats. M26 co-eluted with M3 in the rat fecal profile and, together, these 2 metabolites accounted for 8.2% of the administered dose in rat feces. Several early eluting peaks, before 8 min, and between 15-20 min, in the rat fecal metabolite profile could not be identified because of high mass spectrometric background interference. These unknown peaks comprised 35.6% of the radioactivity in the pooled rat feces (0-168 h). Similar peaks were not observed in the fecal profiles from dog.

Metabolite Profiles in Bile. The parent compound and 13 metabolites were found in the bile from BDC rats (Table 3, Figure 4C). Unchanged parent drug accounted for 5.2% of the dose secreted in the bile of BDC rats. M6, a direct glucuronide conjugate of BMS-690514, was a prominent metabolite in rat bile, accounting for 7.2% of the administered dose. Other prominent biliary metabolites found in rats were M7, M8, and M9, glucuronide conjugates of oxidative metabolites. Interestingly, the early eluting unknown metabolite peaks observed in rat feces were not observed in rat bile.

Downloaded from dmd.aspetjournals.org at ASPET Journals on April 18, 2024

DMD Fast Forward. Published on April 2, 2010 as DOI: 10.1124/dmd.110.032755
This article has not been copyedited and formatted. The final version may differ from this version.

Identification of Metabolites. Metabolites of BMS-690514 were characterized by LC/MS/MS analysis. Similarities in HPLC retention times and mass spectrometric fragmentation patterns to available reference standards facilitated the identification of metabolites M2, M3 and M6. Structures of other metabolites were proposed based on their mass spectrometric fragmentation patterns relative to BMS-690514 or these known metabolites. In addition, the structural assignments of metabolites were further confirmed by high resolution mass spectrometry (Table 4). A list of the metabolites of BMS-690514 found in the *in vivo* samples from rats, rabbits and dogs is complied in Table 4, along with the mass spectrometric fragmentation data supporting the structural characterization of each of the metabolites. Proposed structures and metabolic pathways for the formation of the detected metabolites are shown in Figure 5. Hydroxylated metabolite M1 and the glucuronides, M6, M7 and M8, were isolated from *in vitro* incubations or from rat bile for further characterization by NMR.

The BMS-690514 reference standard had a protonated molecule $[M+H]^+$ of *m/z* 369 and a major MS^2 fragment at *m/z* 253 resulting from cleavage of the carbon-nitrogen bond between the nitrogen of the aminopiperidine ring and the methyl carbon of the methyl pyrrolotriazine group (Table 4). The metabolites of BMS-690514 generally underwent similar fragmentations, enabling structure identification of metabolites by comparison of changes in the masses of fragment ions relative to the parent.

Metabolite M1 had a protonated molecule $[M+H]^+$ of *m/z* 385 (16 Da higher than BMS-690514) and the exact mass measurement suggested that it was a monooxygenated metabolite. The MS^2 spectrum showed major fragment ions of *m/z* 367 (loss of water) and *m/z* 253 (Table 4). M1 was isolated from *in vitro* incubations with human liver

Downloaded from dmd.aspetjournals.org at ASPET Journals on April 18, 2024

DMD Fast Forward. Published on April 2, 2010 as DOI: 10.1124/dmd.110.032755
This article has not been copyedited and formatted. The final version may differ from this version.

microsomes and its identity was confirmed by nuclear magnetic resonance (NMR), a Hydrogen/Deuterium exchange experiment, and high-resolution mass spectrometric analysis. The results from these experiments suggested that M1 was a metabolite that had undergone mono-hydroxylation on the pyrrolotriazine ring and then underwent an intramolecular rearrangement in which the pyrrolotriazine moiety of the parent had rearranged into a pyridotriazine for M1. Detailed experiments conducted to elucidate the structure of M1 will be described in a separate manuscript.

Metabolite M2 is a mono-hydroxylated metabolite of BMS-690514, with the site of hydroxylation on the 3-methoxyaniline group. The reference standard for metabolite M2 had a protonated molecule $[M+H]^+$ of *m/z* 385 (16 Da higher than BMS-690514) and a major MS^2 fragment at *m/z* 269 resulting from cleavage of the nitrogen-carbon bond between the nitrogen of the aminopiperidine ring and the methyl carbon of the methyl pyrrolotriazine group (Table 4). Comparison of the mass spectrometric fragmentation pattern of M2 in biological samples to the authentic M2 reference standard provided additional verification for the identity of M2 in plasma, urine, fecal and bile samples.

Metabolite M3 had a protonated molecule $[M+H]^+$ of *m/z* 355 (14 Da lower than BMS-690514) and the exact mass measurement indicated that it was a demethylated metabolite. The MS^2 spectrum had a major fragment at *m/z* 239, which was 14 Da lower than the corresponding fragment ion of the parent BMS-690514 molecule (*m/z* 253) (Table 4). These data were consistent with a metabolite that had undergone *O*-demethylation of the methyl group on the methoxyaniline moiety.

Metabolite M6 had a protonated molecule $[M+H]^+$ of *m/z* 545 (176 Da higher than

Downloaded from dmd.aspetjournals.org at ASPET Journals on April 18, 2024

DMD Fast Forward. Published on April 2, 2010 as DOI: 10.1124/dmd.110.032755
This article has not been copyedited and formatted. The final version may differ from this version.

BMS-690514) suggesting that it was a direct glucuronide conjugate of the parent molecule. The MS^2 spectra of M6 showed a minor fragment ion at *m/z* 369 (neutral loss of 176 Da, indicative of a glucuronide) and a major fragment ion at *m/z* 253 (Table 4). M6 was isolated from rat bile and the structure was identified by nuclear magnetic resonance. 1D and 2D NMR results showed that chemical shift differences were observed for some of the ^{1}H and ^{13}C atoms of the aminopiperidinal moiety in M6 as compared to the parent compound (Figure 6). Additionally, a key long range ^{1}H-^{13}C correlation between H3 and C29 of the glucuronide was observed and confirmed the attachment site of the glucuronide at position 17 of the parent (Figure 6). The results from these experiments localized the site of glucuronidation on the hydroxyl group of the aminopiperidine moiety.

Metabolites M7, M8 and M27 each had a protonated molecule $[M+H]^+$ of *m/z* 561 (192 Da higher than BMS-690514), and major product ions at *m/z* 269 and *m/z* 385 (neutral loss of 176 Da) (Table 4). The mass spectra indicated that these 3 metabolites are glucuronide conjugates of mono-hydroxylated BMS-690514. The *m/z*-269 fragment was similar to that observed for M2, and suggested that the site of hydroxylation for these metabolites was on the pyrrolotriazine or aniline groups.

M7 and M8 were isolated from rat bile and were further characterized by NMR. Comparison of the chemical shifts of M7 with BMS-690514 revealed several ^{1}H and ^{13}C chemical shift differences, e. g., proton 15 exhibited an upfield shift of 0.32 ppm compared to parent and carbon 15 shifted upfield by 15.7 ppm. More importantly, proton 16 was absent in M7 and carbon 16 has shifted downfield by 21.8 ppm, consistent with the site of hydroxylation on carbon 16 (Figure 6). Key long range ^{1}H-^{13}C correlations

Downloaded from dmd.aspetjournals.org at ASPET Journals on April 18, 2024

DMD Fast Forward. Published on April 2, 2010 as DOI: 10.1124/dmd.110.032755
This article has not been copyedited and formatted. The final version may differ from this version.

were observed between H29 and C16 as well as between H15 and C16 (Figure 6). These correlations and chemical shift changes are consistent with attachment of an ether glucuronide on the C16 of the pyrrolotriazine moiety.

NMR analysis suggested that the isolated M8 peak from rat bile contained two metabolites, M8a and M8b. The two metabolites in the mixture were characterized using 1D and 2D NMR methods. Based on proton integration in the ^{1}H spectrum, M8a was a major component and M8b was a minor component. A proton from the methoxyanaline moiety was absent in the spectra of both metabolites; for M8a, H23 was absent and in metabolite M8b, H25 was absent. Chemical shift differences were also observed for the ^{1}H and ^{13}C atoms of the methoxyanaline moiety. Notably, carbon 23 shifted downfield by 35.9 ppm in M8a and carbon 25 shifted downfield by 28.2 ppm in M8b, suggesting that these carbons are the sites of hydroxylation for M8a and M8b, respectively (Figure 6). Key long range ^{1}H-^{13}C correlations between H29 and C23 in M8a and between H29' and C25' in M8b confirm the site of glucuronidation in both metabolites (Figure 6). For M8a, glucuronidation occurred at the hydroxyl in position 23; for M8b, glucuronidation occurred at the hydroxyl on position 25 (Figure 6).

Metabolites M9 and M28 each had a protonated molecule $[M+H]^{+}$ of *m/z* 531 (176 Da higher than M3). The MS^{2} spectrum of M9 showed major fragment ions at *m/z* 415, 355 (neutral loss of 176), and 239 (Table 4). The fragment at *m/z* 415 resulted from cleavage of the carbon-nitrogen bond between the nitrogen of the aminopiperidine ring and the methyl carbon of the methyl pyrrolotriazine group. The fragment at *m/z* 239 resulted from cleavage of this same bond after loss of the glucuronide moiety. These data suggested M9 is a glucuronide conjugate of M3, with the site of glucuronidation on the pyrrolotriazine

Downloaded from dmd.aspetjournals.org at ASPET Journals on April 18, 2024

DMD Fast Forward. Published on April 2, 2010 as DOI: 10.1124/dmd.110.032755
This article has not been copyedited and formatted. The final version may differ from this version.

or aniline groups. The MS^2 spectrum of M28 showed fragment ions at *m/z* 355 (neutral loss of 176), 293, and 239 (Table 4). The fragments at *m/z* 293 and 239 resulted from cleavage of the carbon-nitrogen bond between the nitrogen of the aminopiperidine ring and the methyl carbon of the methyl pyrrolotriazine group. Particularly, the fragment at *m/z* 293 corresponded to the glucuronidated aminopiperidine moiety. These data suggested that M28 is a glucuronide conjugate of M3, with the site of glucuronidation on the hydroxyaminopiperidine moiety (Figure 5). The exact mass measurement further confirmed that M9 and M28 were glucuronides of demethylated metabolites.

M14 and M36 both had a protonated molecule $[M+H]^+$ of *m/z* 547, which was 192 Da higher than M3 and MS^2 fragment ions at *m/z* 431, 371 (loss of 176 Da), and 255 (Table 4). The fragment at *m/z* 431 resulted from cleavage of the carbon-nitrogen bond between the nitrogen of the aminopiperidine ring and the methyl carbon of the methyl pyrrolotriazine group. The fragment at *m/z* 255 resulted from cleavage of this same bond after loss of the glucuronide moiety and it was 16 Da higher than *m/z* 239, which was the corresponding fragment of M3. These data suggest that M14 and M36 are glucuronide conjugates of monooxygenated M3 and these proposed structures were supported by the results of exact mass measurement.

M24 had a protonated molecule $[M+H]^+$ of *m/z* 589, which was 220 Da higher than BMS-690514. The MS^2 spectrum of M24 showed major fragment ions at *m/z* 413 (neutral loss of 176), and 253 (Table 4). The fragment at *m/z* 413 (44 Da higher than the $[M+H]^+$ of the parent molecule) and fragment at *m/z* 253 (same fragment as the parent molecule), suggested that a carboxylation had occurred on the aminopiperidine moiety.

Downloaded from dmd.aspetjournals.org at ASPET Journals on April 18, 2024

DMD Fast Forward. Published on April 2, 2010 as DOI: 10.1124/dmd.110.032755
This article has not been copyedited and formatted. The final version may differ from this version.

After treatment with β-glucuronidase, M24 was completely hydrolyzed and converted to BMS-690514 (Figure 7A and 7B), which confirmed that M24 was a glucuronide metabolite. Although the carbamic acid intermediate was not observed in the incubation mixture by LC-MS/MS due to the instability of this species (Shaffer et al., 2005; Gunduz et al., 2010), the fragmentation of M24 has the signature fragmentation pattern of *N*-carbamoyl glucuronides, which produced the product ion of *m/z* 413, 44 Da higher than the parent drug (Dow et al., 1994; Liu et al., 2001; Shaffer et al., 2005; Gunduz et al., 2010). The exact mass measurement confirmed that M24 is a carbamoyl glucuronide of BMS-690514 (Figure 7C and Figure 7D).

M26 had a protonated molecule $[M+H]^+$ of *m/z* 385 (16 Da higher than BMS-690514) and the exact mass measurement suggested that it was a monooxygenated metabolite. The major MS^2 fragment at *m/z* 269 further suggested that the addition of 16 Da had occurred on the pyrrolotriazine or aniline groups (Table 4).

M30 had a protonated molecule $[M+H]^+$ of *m/z* 367 (2 Da lower than BMS-690514). The exact mass measurement suggested a formula with the loss of two hydrogen atoms from the parent. A major MS^2 fragment ion at *m/z* 269, that was 16 Da higher than the corresponding fragment ion from BMS-690514 (*m/z* 253) suggested that an addition of 16 Da had occurred on the pyrrolotriazine or aniline groups (Table 4). A structure consistent with these data is one in which a monooxygenation (M+16) occurred on the pyrrolotriazine or aniline groups, and a dehydration (M-18) occurred on the aminopiperidine moiety.

M32 had a protonated molecule $[M+H]^+$ of *m/z* 371 (16 Da higher than M3) and a major

Downloaded from dmd.aspetjournals.org at ASPET Journals on April 18, 2024

DMD Fast Forward. Published on April 2, 2010 as DOI: 10.1124/dmd.110.032755
This article has not been copyedited and formatted. The final version may differ from this version.

MS^2 fragment ion at *m/z* 255 (Table 4). The fragment at *m/z* 255 was 16 Da higher than the corresponding fragment ion of M3, suggesting that the site of modification was on the pyrrolotriazine or aniline groups. These data are consistent with a metabolite that had undergone *O*-demethylation (M-14) and monooxygenation (M+16) on the pyrrolotriazine or aniline groups. This purposed structure has a consistent molecular formula with the one suggested by the exact mass measurement.

M35 had a protonated molecule $[M+H]^+$ of *m/z* 383 (2 Da less than M2) and a major MS^2 fragment ion at *m/z* 269 (Table 4). The result of exact mass measurement suggested an addition of oxygen atom and loss of two hydrogen atoms from the parent molecule. The fragment at *m/z* 269 was the same as the corresponding fragment ion of M2, suggested an addition of oxygen occurred on the on the pyrrolotriazine or aniline groups. A structure consistent with these data is one in which an M+16 oxidation occurred on the pyrrolotriazine or aniline groups, and a dehydrogenation (M-2) occurred on the aminopiperidine moiety.

M37 had a protonated molecule $[M+H]^+$ of *m/z* 385 (16 Da higher than BMS-690514) and a major MS^2 fragment at *m/z* 269, suggesting that the addition of 16 Da had occurred on the pyrrolotriazine or aniline groups (Table 4). M37 and M2 coeluted on the HPLC and had similar MS and MS^2 spectra. Incubation of human liver microsomes with deuterated BMS-690514 (labeled on the 16 position) generated unlabeled M37, suggesting that M37 was hydroxylated at the 16 position and the deuterium label at this position was lost upon the formation of M37. The experimental details conducted to elucidate the structure of M37 will be described in a separate manuscript.

Downloaded from dmd.aspetjournals.org at ASPET Journals on April 18, 2024

DMD Fast Forward. Published on April 2, 2010 as DOI: 10.1124/dmd.110.032755
This article has not been copyedited and formatted. The final version may differ from this version.

Discussion

The objectives of the current studies were to evaluate the metabolism and disposition of [^{14}C]BMS-690514 in rat and dog, two species used in long term toxicology studies. In addition, circulating levels of parent compound and metabolites were quantified in these species and in rabbit, an additional investigative species.

Earlier studies demonstrated that formation of M6, a glucuronide conjugate, was an important pathway for biotransformation of BMS-690514 in hepatocyte preparations from various species (Marathe et al., 2010). Therefore, besides intact rat and dog studies, this studies included an assessment of bile from BDC rats after administration of [^{14}C]BMS-690514, to understand the role of conjugative metabolism in the disposition of BMS-690514 as well as the possible contribution of biliary secretion of parent drug.

Following administration of a single oral dose of [^{14}C]BMS-690514, the recovery of radioactivity was 95.4% and 89.6%, in intact rats and dogs, respectively, indicating good mass balance (Table 1). In both species, the majority of the administered radioactivity (>60%), was recovered in the feces. After oral administration of [^{14}C]BMS-690514 to BDC rats, approximately 83% and 17% of the dose was recovered in bile and urine, respectively, suggesting that BMS-690514 was well absorbed in rats. The parent compound comprised <12% of the radioactive dose recovered in the excreta from intact and BDC rats and dogs, suggesting that BMS-690514 was primarily cleared by metabolism in these species.

Pharmacokinetic profiles of total radioactivity and BMS-690514 from rat, rabbit and dog plasma (Figure 2A-C), suggested that metabolites contributed substantially to the AUC of

Downloaded from dmd.aspetjournals.org at ASPET Journals on April 18, 2024

DMD Fast Forward. Published on April 2, 2010 as DOI: 10.1124/dmd.110.032755
This article has not been copyedited and formatted. The final version may differ from this version.

total radioactivity over the 0-8 h interval. Consistently, the metabolite profiles from the 2-h plasma samples (Figure 2A-C, Table 2) confirmed that for all species, particularly for rabbit and dog, multiple metabolites contributed a large portion of the plasma radioactivity at that time point. The metabolite profiles in plasma from rats, rabbits and dogs were qualitatively similar (Figures 3A-C). In all species, BMS-690514 and multiple oxidative and conjugative metabolites were detected in the plasma; M1, a hydroxylated metabolite, M6, a direct glucuronide conjugate, and M7, M8 and M9, glucuronide conjugates of oxidative metabolites were prominent circulating metabolites in all species. The parent compound was the predominant peak in rat plasma, and rat tended to have a greater abundance of oxidative metabolites (M1, M3 and M26) in the circulation than other species. In rabbits and dogs, glucuronides M6-M9 were the most prominent plasma metabolites. In the plasma metabolite profiles from intact rat, there was a prominent, but unidentified component which eluted at approximately 26 min (unknown, Figure 3A). This peak was present in the 1-8 h plasma samples from intact rats, but it was not present in the plasma profiles from BDC rats (not shown), rabbits or dogs, nor was it present in the bile, urine or fecal profiles from rats, rabbits or dogs. The mass spectrum of the unknown peak did not show a distinct protonated molecule. In addition, no drug-related component was detected under the unknown peak when the rat plasma sample was analyzed on a LTQ-Orbitrap under either positive or negative ionization modes, even after processing the data with a mass-defect filter (Zhang et al., 2003; Zhang et al., 2009). It is possible that the radioactive component in the unknown peak was not readily ionized under the mass spectrometric conditions used in these experiments.

Downloaded from dmd.aspetjournals.org at ASPET Journals on April 18, 2024

DMD Fast Forward. Published on April 2, 2010 as DOI: 10.1124/dmd.110.032755
This article has not been copyedited and formatted. The final version may differ from this version.

Approximately 5% of the administered dose was excreted as unchanged parent compound in rat bile after oral administration of [^{14}C]BMS-690514. Glucuronide conjugates of the parent (M6) and oxidative metabolites (M7-9, M27 and M28) accounted for another 31.8% of the dose in the rat bile. Glucuronide conjugated metabolites also comprised the majority of the biliary radioactivity after oral administration of [^{3}H]BMS-690514 to BDC dogs (data not shown). In contrast, BMS-690514 and oxidative metabolites comprised most of the excreted dose in the feces of intact rats and dogs and little to no glucuronide metabolites were detected (Figure 4, Table 3). The difference in the bile and fecal profiles was attributed to hydrolysis of the conjugative metabolites in the gastrointestinal tract before excretion in the feces (Parker et al., 1980; Christopher et al., 2008). M6, which was hydrolyzed in the gastrointestinal tract, could be re-absorbed as the parent compound, leading to further oxidative metabolism. These data suggested that oxidative metabolism may ultimately be the primary clearance pathway for BMS-690514, even though glucuronide conjugates were responsible for the majority of the biliary radioactivity in BDC rats and dogs.

These results demonstrate the importance of collecting and profiling bile to understand the complete disposition of a compound, such as BMS-690514, which has a significant amount of conjugated metabolites excreted via the bile. Bile collection may also provide insight for other biotransformations. For example, several unidentified peaks observed in rat feces were not present in rat bile. These data suggest that the unknown compounds were likely generated by microflora residing in the gastrointestinal tract of the rat. Without bile data, these peaks would have been attributed to systemic metabolism.

Together, the fecal and bile metabolite profiles suggested that the primary *in vivo*

Downloaded from dmd.aspetjournals.org at ASPET Journals on April 18, 2024

DMD Fast Forward. Published on April 2, 2010 as DOI: 10.1124/dmd.110.032755
This article has not been copyedited and formatted. The final version may differ from this version.

metabolic pathways of BMS-690514 in all species were hydroxylation to form M1, M2 and M37, *O*-demethylation to form M3, and direct glucuronidation to form M6, which were in good agreement with the *in vitro* hepatocyte data (Marathe et al., 2010). In human hepatocytes, along with M1 and M3 formed through oxidative pathway, direct glucuronide metabolite M6 was also formed (Marathe et al., 2010), suggesting that these pathways are also likely to be important *in vivo* metabolic pathways in humans (Figure 5). In addition, the presence of these metabolites *in vivo* in animals suggested that these toxicology species, rats, dogs and rabbits, were exposed to human relevant metabolites.

M2 was a mono-hydroxylated metabolite of BMS-690514, with the site of hydroxylation on the 3-methoxyaniline group in a position that is para to the amino group. Studies have suggested that some drugs containing a hydroxylaniline group may be bioactivated to form a quinone imine, which is capable of reacting with glutathione (GSH) or nucleophilic groups in proteins (Kalgutkar et al., 2005a; Kalgutkar et al., 2005b; Madsen et al., 2008; Li et al., 2009). Furthermore, this CYP-dependent bioactivation may also result in mechanism-based inactivation of CYP enzymes (Kalgutkar et al., 2005b; Li et al., 2009). Although a time-dependent inhibition study of CYP enzymes has not been conducted for BMS-690514, the current data showed that no GSH adducts, cysteine adducts or quinone imine metabolites were identified in any samples collected in the *in vivo* studies. In addition, no GSH conjugates of BMS-690514 were found in the *in vitro* incubations of BMS-690514 with GSH-supplemented rat or human liver S9 fractions (data not shown). Good extraction recovery of drug-related radioactivity was observed from plasma samples from rats, rabbits or dogs after p.o. administration of [^{14}C]BMS-690514. Therefore, the mechanism-based inactivation of CYP enzymes by BMS-690514

Downloaded from dmd.aspetjournals.org at ASPET Journals on April 18, 2024

DMD Fast Forward. Published on April 2, 2010 as DOI: 10.1124/dmd.110.032755
This article has not been copyedited and formatted. The final version may differ from this version.

due to the bioactivation of M2 through the quinone imine pathway is not anticipated. In addition, BMS-690514 showed little potential to inhibit CYP enzymes in competitive inhibition assays, which included an evaluation of CYP3A4 and CYP2D6, two of the key CYP enzymes involved in the metabolism of BMS-690514 (Marathe et al., 2010).

M1 and M37 were both hydroxylated metabolites with hydroxyl group on the 16 position of the molecule. M37 generated from deuterated BMS-690514 (labeled on the 16 position) completely lost the isotope label, while M1 generated from the same deuterated BMS-690514 retained the deuterium label on the original site (data not shown), suggesting that M37 was not an intermediate of M1. Detailed experiments conducted to elucidate the exact structure of M1 and the mechanism for the formation of M1 and M37 will be described in a separate manuscript. It should be noted that due to well characterized impacts of isotope substitution at sites of CYP-mediated metabolism (Nelson and Trager, 2003), the substitution of deuterium at that position would affect the biotransformation and possibly impact the kinetics of clearance of BMS-690514.

BMS-690514 contains an *m*-anisidine (3-methoxyaniline) moiety. Anisidine isomers are known to be toxic (1978a; 1978b; Thompson and Eling, 1991). Therefore we considered the possibility that *m*-anisidine group may be released from BMS-690514 after p.o. administration. No *m*-anisidine was detected in the plasma or excreta samples from any of the species, suggesting that the toxicity through this pathway is unlikely to be seen *in vivo*.

In summary, this investigation demonstrated that BMS-690514 was well absorbed and cleared primarily by metabolism in rats and dogs. Biliary secretion was the major route

Downloaded from dmd.aspetjournals.org at ASPET Journals on April 18, 2024

DMD Fast Forward. Published on April 2, 2010 as DOI: 10.1124/dmd.110.032755
This article has not been copyedited and formatted. The final version may differ from this version.

for elimination of drug-related radioactivity in BDC rats. The primary *in vivo* metabolic pathways for BMS-690514 in rats, rabbits and dogs were hydroxylation to form M1, M2 and M37, *O*-demethylation to form M3, and direct glucuronidation to form M6, which was similar to the *in vitro* metabolism of BMS-690514 observed in hepatocyte incubations from various animal species and humans. The major metabolic and clearance pathways in the preclinial species studied here are likely to be the same as those in humans, thus confirming the suitability of these species for the toxicity assessments of BMS-690514.

Downloaded from dmd.aspetjournals.org at ASPET Journals on April 18, 2024

DMD Fast Forward. Published on April 2, 2010 as DOI: 10.1124/dmd.110.032755
This article has not been copyedited and formatted. The final version may differ from this version.

References

(1978a) Bioassay of o-anisidine hydrochloride for possible carcinogenicity. *Natl Cancer Inst Carcinog Tech Rep Ser* **89:**1-149.

(1978b) Bioassay of p-Anisidine Hydrochloride for Possible Carcinogenicity (CAS No. 20265-97-8). *Natl Cancer Inst Carcinog Tech Rep Ser* **116:**1-115.

Bahleda R, Felip E, Herbst RS, Hanna NH, Laurie SA, Shepherd FA, Armand JP, Sweeney CJ, Calvo-Aller E and Soria JC (2008) Phase I multicenter trial of BMS-690514: Safety, pharmacokinetic profile, biological effects, and early clinical evaluation in patients with advanced solid tumors and non-small cell lung cancer. *J Clin Oncol* **26:**2584.

Bahleda R, Soria J, Harbison C, Park J, E. Felip, Hanna N, Laurie SA, Armand J, Shepherd FA and Herbst R (2009) Tumor regression and pharmacodynamic (PD) biomarker validation in non-small cell lung cancer (NSCLC) patients treated with the ErbB/VEGFR inhibitor BMS-690514., in: *J Clin Oncol*, pp abstr 8098.

Christopher LJ, Cui D, Li W, Barros A, Jr., Arora VK, Zhang H, Wang L, Zhang D, Manning JA, He K, Fletcher AM, Ogan M, Lago M, Bonacorsi SJ, Humphreys WG and Iyer RA (2008) Biotransformation of [^{14}C]dasatinib: in vitro studies in rat, monkey, and human and disposition after administration to rats and monkeys. *Drug Metab Dispos* **36:**1341-1356.

de La Motte Rouge T, Galluzzi L, Olaussen KA, Zermati Y, Tasdemir E, Robert T, Ripoche H, Lazar V, Dessen P, Harper F, Pierron G, Pinna G, Araujo N, Harel-Belan A, Armand JP, Wong TW, Soria JC and Kroemer G (2007) A novel

Downloaded from dmd.aspetjournals.org at ASPET Journals on April 18, 2024

DMD Fast Forward. Published on April 2, 2010 as DOI: 10.1124/dmd.110.032755
This article has not been copyedited and formatted. The final version may differ from this version.

epidermal growth factor receptor inhibitor promotes apoptosis in non-small cell lung cancer cells resistant to erlotinib. *Cancer Res* **67:**6253-6262.

Dow J, Piriou F, Wolf E, Dulery BD and Haegele KD (1994) Novel carbamate metabolites of mofegiline, a primary amine monoamine oxidase B inhibitor, in dogs and humans. *Drug Metab Dispos* **22:**738-749.

Fukuoka M, Yano S, Giaccone G, Tamura T, Nakagawa K, Douillard JY, Nishiwaki Y, Vansteenkiste J, Kudoh S, Rischin D, Eek R, Horai T, Noda K, Takata I, Smit E, Averbuch S, Macleod A, Feyereislova A, Dong RP and Baselga J (2003) Multi-institutional randomized phase II trial of gefitinib for previously treated patients with advanced non-small-cell lung cancer. *J Clin Oncol* **21:**2237-2246.

Gunduz M, Algikar U, Baeschlin D, Ferreira S, Hosagrahara V and Harriman S (2010) Identification of a novel *N*-carbamoyl glucuronide: in vitro, in vivo, and mechanistic studies. *Drug Metab Dispos* **38:**361-367.

Herbst RS, Johnson DH, Mininberg E, Carbone DP, Henderson T, Kim ES, Blumenschein G, Jr., Lee JJ, Liu DD, Truong MT, Hong WK, Tran H, Tsao A, Xie D, Ramies DA, Mass R, Seshagiri S, Eberhard DA, Kelley SK and Sandler A (2005) Phase I/II trial evaluating the anti-vascular endothelial growth factor monoclonal antibody bevacizumab in combination with the HER-1/epidermal growth factor receptor tyrosine kinase inhibitor erlotinib for patients with recurrent non-small-cell lung cancer. *J Clin Oncol* **23:**2544-2555.

Kalgutkar AS, Henne KR, Lame ME, Vaz AD, Collin C, Soglia JR, Zhao SX and Hop CE (2005a) Metabolic activation of the nontricyclic antidepressant trazodone to

Downloaded from dmd.aspetjournals.org at ASPET Journals on April 18, 2024

DMD Fast Forward. Published on April 2, 2010 as DOI: 10.1124/dmd.110.032755
This article has not been copyedited and formatted. The final version may differ from this version.

electrophilic quinone-imine and epoxide intermediates in human liver microsomes and recombinant P4503A4. *Chem Biol Interact* **155:**10-20.

Kalgutkar AS, Vaz AD, Lame ME, Henne KR, Soglia J, Zhao SX, Abramov YA, Lombardo F, Collin C, Hendsch ZS and Hop CE (2005b) Bioactivation of the nontricyclic antidepressant nefazodone to a reactive quinone-imine species in human liver microsomes and recombinant cytochrome P450 3A4. *Drug Metab Dispos* **33:**243-253.

Kris MG, Natale RB, Herbst RS, Lynch TJ, Jr., Prager D, Belani CP, Schiller JH, Kelly K, Spiridonidis H, Sandler A, Albain KS, Cella D, Wolf MK, Averbuch SD, Ochs JJ and Kay AC (2003) Efficacy of gefitinib, an inhibitor of the epidermal growth factor receptor tyrosine kinase, in symptomatic patients with non-small cell lung cancer: a randomized trial. *JAMA* **290:**2149-2158.

Li X, He Y, Ruiz CH, Koenig M and Cameron MD (2009) Characterization of dasatinib and its structural analogs as CYP3A4 mechanism-based inactivators and the proposed bioactivation pathways. *Drug Metab Dispos* **37:**1242-1250.

Liu DQ, Hop CE, Beconi MG, Mao A and Chiu SH (2001) Use of on-line hydrogen/deuterium exchange to facilitate metabolite identification. *Rapid Commun Mass Spectrom* **15:**1832-1839.

Madsen KG, Gronberg G, Skonberg C, Jurva U, Hansen SH and Olsen J (2008) Electrochemical oxidation of troglitazone: identification and characterization of the major reactive metabolite in liver microsomes. *Chem Res Toxicol* **21:**2035-2041.

Downloaded from dmd.aspetjournals.org at ASPET Journals on April 18, 2024

DMD Fast Forward. Published on April 2, 2010 as DOI: 10.1124/dmd.110.032755
This article has not been copyedited and formatted. The final version may differ from this version.

Marathe P, Tang W, Sleczka B, Rodrigues D, Gavai A, Wong T, Christopher L and Zhang H (2010) Preclincal pharmacokinetics and in vitro metabolism of BMS-690514, a potent inhibitor of EGFR and VEGFR2. *J. Pharm. Sci.* (DOI 10.1002/jps.22099)

Nelson SD and Trager WF (2003) The use of deuterium isotope effects to probe the active site properties, mechanism of cytochrome P450-catalyzed reactions, and mechanisms of metabolically dependent toxicity. *Drug Metab Dispos* **31:**1481-1498.

Parker RJ, Hirom PC and Millburn P (1980) Enterohepatic recycling of phenolphthalein, morphine, lysergic acid diethylamide (LSD) and diphenylacetic acid in the rat. Hydrolysis of glucuronic acid conjugates in the gut lumen. *Xenobiotica* **10:**689-703.

Reck M, von Pawel J, Zatloukal P, Ramlau R, Gorbounova V, Hirsh V, Leighl N, Mezger J, Archer V, Moore N and Manegold C (2009) Phase III trial of cisplatin plus gemcitabine with either placebo or bevacizumab as first-line therapy for nonsquamous non-small-cell lung cancer: AVAiL. *J Clin Oncol* **27:**1227-1234.

Sandler A, Gray R, Perry MC, Brahmer J, Schiller JH, Dowlati A, Lilenbaum R and Johnson DH (2006) Paclitaxel-carboplatin alone or with bevacizumab for non-small-cell lung cancer. *N Engl J Med* **355:**2542-2550.

Shaffer CL, Gunduz M, O'Connell TN, Obach RS and Yee S (2005) Biotransformation of a GABAA receptor partial agonist in sprague-dawley rats and cynomolgus monkeys: identification of two unique N-carbamoyl metabolites. *Drug Metab Dispos* **33:**1688-1699.

Downloaded from dmd.aspetjournals.org at ASPET Journals on April 18, 2024

DMD Fast Forward. Published on April 2, 2010 as DOI: 10.1124/dmd.110.032755
This article has not been copyedited and formatted. The final version may differ from this version.

Shepherd FA, Rodrigues Pereira J, Ciuleanu T, Tan EH, Hirsh V, Thongprasert S, Campos D, Maoleekoonpiroj S, Smylie M, Martins R, van Kooten M, Dediu M, Findlay B, Tu D, Johnston D, Bezjak A, Clark G, Santabarbara P and Seymour L (2005) Erlotinib in previously treated non-small-cell lung cancer. *N Engl J Med* **353:**123-132.

Tabernero J (2007) The role of VEGF and EGFR inhibition: implications for combining anti-VEGF and anti-EGFR agents. *Mol Cancer Res* **5:**203-220.

Thompson DC and Eling TE (1991) Reactive intermediates formed during the peroxidative oxidation of anisidine isomers. *Chem Res Toxicol* **4:**474-481.

Tortora G, Ciardiello F and Gasparini G (2008) Combined targeting of EGFR-dependent and VEGF-dependent pathways: rationale, preclinical studies and clinical applications. *Nat Clin Pract Oncol* **5:**521-530.

Wong T, Ayers M and Emanuel S (2007) Inhibition of EGFR/HER2 signaling in tumor cells and VEGFR2 activity in tumor endothelium contribute to the preclinical anti-tumor activity of BMS-690514., in: *AACR Meeting Abstracts*, pp 4007.

Zhang H, Zhang D and Ray K (2003) A software filter to remove interference ions from drug metabolites in accurate mass liquid chromatography/mass spectrometric analyses. *J Mass Spectrom* **38:**1110-1112.

Zhang H, Zhang D, Ray K and Zhu M (2009) Mass defect filter technique and its applications to drug metabolite identification by high-resolution mass spectrometry. *J Mass Spectrom* **44:**999-1016.

Downloaded from dmd.aspetjournals.org at ASPET Journals on April 18, 2024

DMD Fast Forward. Published on April 2, 2010 as DOI: 10.1124/dmd.110.032755
This article has not been copyedited and formatted. The final version may differ from this version.

Figure Legends

Figure 1. Structure of [^{14}C]BMS-690514. The compound was uniformly labeled on the six carbons of methoxyaniline ring.

Figure 2. Plasma concentration of total radioactivity (•) and BMS-690514 (◦) versus time after p.o. administration of [^{14}C]BMS-690514 to A) rats, B) rabbits and C) dogs and D) Summary of AUC (0-8 h) values for BMS-690514 and total radioactivity in rats, rabbits and dogs.

Figure 3. Representative biotransformation profile of pooled plasma samples collected at 2 h after p.o. administration of [^{14}C]BMS-690514 to A) rats, B) rabbits, and C) dogs

Figure 4. Biotransformation profiles of pooled A) urine, B) feces and C) bile from rats and D) urine and E) feces from dogs after administration of a single oral dose of [^{14}C]BMS-690514. The urine and fecal profiles were obtained from intact rats and dogs in the 0-168 h interval after dose administration. The bile profile was obtained from BDC rats in the 0-24-h interval post-dose.

Figure 5. Proposed biotransformation pathways of BMS-690514 in rats, rabbits and dogs. Pathways were proposed based on metabolites found in *in vivo* plasma, bile, urine, and fecal samples collected from the three animal species administered a single dose of [^{14}C]BMS-690514.

Figure 6. Structures of metabolites M6, M7 and M8 (M8a and M8b) of BMS-690514. A) Key HMBC correlations for structure identification (labeled with arrows); B) Key NMR

Downloaded from dmd.aspetjournals.org at ASPET Journals on April 18, 2024

DMD Fast Forward. Published on April 2, 2010 as DOI: 10.1124/dmd.110.032755
This article has not been copyedited and formatted. The final version may differ from this version.

chemical shift data for BMS-690514 and metabolites M6, M7, M8a and M8b. Atom numbers are for illustrative purposes and do not conform to International Union of Pure and Applied Chemistry nomenclature.

Figure 7. LC-high resolution mass spectrometric analysis of M24 before and after treatment with β-glucuronidase. A) LC-MS chromatogram of M24 before treatment with β-glucuronidase; B) LC-MS chromatogram of M24 after treatment with β-glucuronidase; M24 was completely converted to BMS-690514 by β-glucuronidase, indicating M24 was a glucuronide; C and D) High resolution mass spectrum of protonated M24 and MS/MS spectrum of M24. The molecular formula of M24 and the fragmentation of M24 suggested by the high resolution mass spectrometric data confirmed that M24 was an *N*-carbamoyl glucuronide. The mass accuracy was within 2 ppm.

Downloaded from dmd.aspetjournals.org at ASPET Journals on April 18, 2024

Table 1. Percentage of dose recovered following administration of a single oral dose of [^{14}C]BMS-690514 to rats and dogs

Species	Dose (mg/kg)	Collection Interval (h)	Percentage of Dose Recovered					
			Urine	Feces	Bile	Cage Debris/Wash	Carcass	Total
Rat	15	0-168	18.40 ± 1.12	71.19 ± 5.55	NA	5.44 ± 6.09	0.40 ± 0.07	95.43 ± 2.89
BDC Rat	15	0-24	17.13 ± 3.89	5.77 ± 2.93	83.37 ± 6.08	1.01 ± 0.46	NA	107.3 ± 1.73
Dog	10	0-168	20.12 ± 3.76	60.78 ± 11.82	NA	8.67 ± 7.45	NA	89.57 ± 4.67

Downloaded from dmd.aspetjournals.org at ASPET Journals on April 18, 2024

DMD Fast Forward. Published on April 2, 2010 as DOI: 10.1124/dmd.110.032755
This article has not been copyedited and formatted. The final version may differ from this version.

DMD Fast Forward. Published on April 2, 2010 as DOI: 10.1124/dmd.110.032755
This article has not been copyedited and formatted. The final version may differ from this version.

Table 2. Relative abundance of BMS-690514 and metabolites in pooled plasma samples collected 2 h after administration of a single oral dose of [^{14}C]BMS-690514 to rats, rabbits and dogs

Metabolite ID[a]	Percent of sample radioactivity		
	Rats	**Rabbit**	**Dogs**
M1	3.1	5.3	2.5
M3/M26	5.5[b]	ND	ND
M6	ms	2.6	24.8
M7/M9	3.3[c]	14.8[c]	40.0[c]
M8	2.6	60.8	5.4
M14	ms	1.4	2.8
M27	ND	0.8	ND
M28	ms	0.8	ms
M35	ND	2.0	ND
M36	ND	1.2	ND
Parent	56.9	7.3	18.4
Unknown	19.4	ND	ND
Total[d]	90.8	97.0	93.9

[a] Structures of metabolites are shown in Figure 5.

[b] Metabolites M3 and M26 were identified by mass-spectrometry in the plasma samples from rats, but co-eluted in HPLC.

[c] Metabolites M7 and M9 co-eluted on the HPLC, but could be differentiated by mass-spectrometry in the plasma samples from rats, dogs and rabbits.

[d] The total sample radioactivity (sum of radioactive peaks) was less than 100% due to the presence of several small unidentified radioactive peaks that were present in the radioprofiles. Each of the unidentified peaks accounted for <2.8% of the plasma radioactivity.

Abbreviations ND = not detected by radioactivity or by mass spectrometry; ms = metabolite was detected by mass spectrometry but not by radioactivity.

Downloaded from dmd.aspetjournals.org at ASPET Journals on April 18, 2024

DMD Fast Forward. Published on April 2, 2010 as DOI: 10.1124/dmd.110.032755
This article has not been copyedited and formatted. The final version may differ from this version.

Table 3. Percentage of dose excreted as BMS-690514 and metabolites in pooled urine and feces after administration of a single oral dose of [^{14}C]BMS-690514 to intact rats and dogs or urine and bile after administration of a single oral dose of [^{14}C]BMS-690514 to bile duct-cannulated rats

Metabolite ID[a]	Percentage of Dose					
	Rats[b]		BDC-Rats[b]		Dogs[b]	
	Urine	Feces	Urine	Bile	Urine	Feces
M1	ND	ND	ND	8.6	ND	ND
M2/M37[c]	3.5	6.9	4.2	0.9	0.4	15.6
M3/M26[d]	4.0	8.2	6.7	4.0	1.2	16.3
M6	ND	ND	0.3	7.2	2.9	4.8
M7/M9[e]	0.5	ND	0.5	14.2	6.5	ND
M8	0.4	ND	0.6	9.8	1.4	ND
M24	ND	ND	ND	2.0	ND	ND
M27	ND	ND	ND	0.6	0.2	ND
M28	ND	ND	ND	ND	0.3	ND
M30	ND	ND	ND	2.8	ND	ND
M32	ND	ND	ND	2.2	ND	ND
P	5.0	6.8	2.3	5.2	1.0	2.3
Total	13.4	21.9	14.6	57.5	13.9	39.1

[a] Structures of metabolites are shown in Figure 5.

[b] The urine and feces samples from rats and dogs were collected from 0-168 h after dosing; and the urine and bile from BDC-rats were collected from 0-24 h after dosing.

[c] Metabolites M2 and M37 are known to co-elute on the HPLC and also have similar mass spectrometric characteristics. Both metabolites were detected in incubations of deuterated BMS-690514 with human liver microsomes and are probably co-eluting in these excreta samples. The relative contributions of these two metabolites could not be determined.

[d] Metabolites M3 and M26 co-eluted on the HPLC, but could be differentiated by mass-spectrometry in the urine and fecal samples from rats and in the urine and bile samples from BDC-rats. M26 was not detected by mass-spectrometry in the urine and fecal samples from dogs.

[e] Metabolites M7 and M9 co-eluted on the HPLC but could be differentiated by mass-spectrometry in the urine samples from rats, BDC rats and dogs and in the bile from BDC-rats.

Abbreviation: ND = not detected by radioactivity

Downloaded from dmd.aspetjournals.org at ASPET Journals on April 18, 2024

Table 4. Mass spectrometric characterization of BMS-690514 metabolites identified from plasma, urine, bile and feces samples collected after administration of [^{14}C]BMS-690514 to rats, dogs and rabbits.

BMS-690514 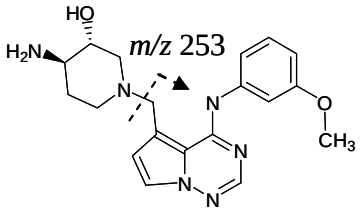	M1 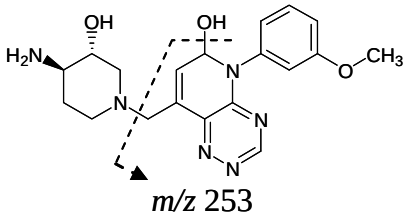	M2 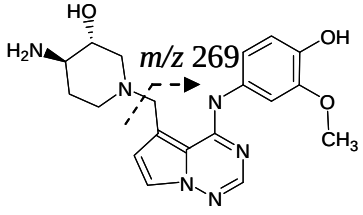
M3 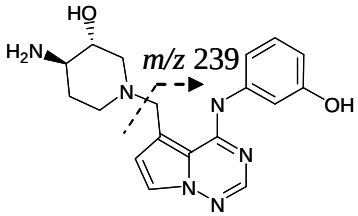	M6 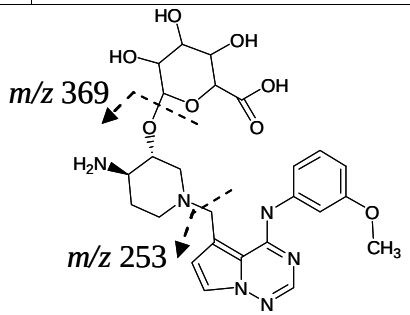	

Metabolite	[M + H]$^{+}$ [a]	Proposed Formula	Major Fragment Ions[b]	Metabolic Pathway (s)	Animal Species		
P	369.2029	$C_{19}H_{25}O_2N_6$	253		Rat	Rabbit	Dog
M1	385.1978	$C_{19}H_{25}O_3N_6$	253, <u>367</u>	Hydroxylation, rearrangement	Rat	Rabbit	Dog
M2[b]	385.1976	$C_{19}H_{25}O_3N_6$	<u>269</u>, 237	Hydroxylation	Rat		Dog
M3	355.1872	$C_{18}H_{23}O_2N_6$	239	*O*-demethylation	Rat		Dog
M6	545.2344	$C_{25}H_{33}O_8N_6$	369, <u>253</u>	Glucuronidation	Rat	Rabbit	Dog

Downloaded from dmd.aspetjournals.org at ASPET Journals on April 18, 2024

DMD Fast Forward. Published on April 2, 2010 as DOI: 10.1124/dmd.110.032755
This article has not been copyedited and formatted. The final version may differ from this version.

M7	561.2294	$C_{25}H_{33}O_9N_6$	269, 385, 445,	Hydroxylation, glucuronidation	Rat	Rabbit	Dog
M8	561.2292	$C_{25}H_{33}O_9N_6$	269, 385, 445	Hydroxylation, glucuronidation	Rat	Rabbit	Dog
M9	531.2187	$C_{24}H_{31}O_8N_6$	239, 355, 415	*O*-demethylation, glucuronidation	Rat	Rabbit	Dog
M14	547.2138	$C_{24}H_{31}O_9N_6$	255, 371, 431	Monooxygenation, *O*-demethylation, glucuronidation		Rabbit	Dog
M24	589.2243	$C_{26}H_{33}O_{10}N_6$	253, 413	Carbamoylation, glucuronidation	Rat		
M26	385.1978	$C_{19}H_{25}O_3N_6$	269	Monooxygenation	Rat		
M27	561.2296	$C_{25}H_{33}O_9N_6$	237, 269, 385	Hydroxylation, glucuronidation	Rat	Rabbit	Dog
M28	531.2188	$C_{24}H_{31}O_8N_6$	239, 293, 355	*O*-demethylation, glucuronidation	Rat	Rabbit	Dog
M30	367.1873	$C_{19}H_{23}O_2N_6$	241, 253, 269	Monooxygenation, dehydration	Rat		
M32	371.1821	$C_{18}H_{23}O_3N_6$	255	Monooxygenation, *O*-demethylation	Rat		

Downloaded from dmd.aspetjournals.org at ASPET Journals on April 18, 2024

DMD Fast Forward. Published on April 2, 2010 as DOI: 10.1124/dmd.110.032755
This article has not been copyedited and formatted. The final version may differ from this version.

M35	383.1820	$C_{19}H_{23}O_3N_6$	269, 365, <u>366</u>	Monooxygenation, dehydrogenation		Rabbit	
M36	547.2134	$C_{24}H_{31}O_9N_6$	<u>255</u>, 371, 431	Monooxygenation, *O*-demethylation, glucuronidation		Rabbit	
M37[c]	385.1978	$C_{19}H_{25}O_3N_6$	<u>269</u>, 237	Hydroxylation	Rat	Rabbit	Dog

[a] The *m/z* values of protonated molecules were measured on an LTQ-Orbitrap. The mass accuracy for all measurements was within 3 ppm of the theoretical values.

[b] The most abundant peak in MS/MS spectra are underlined.

[c] Metabolites M2 and M37 are known to co-elute on the HPLC and also have similar mass spectrometric characteristics. Both metabolites were detected in incubations of deuterated BMS-690514 with human liver microsomes and are likely present in the in vivo samples from all 3 species, since glucuronides of these metabolites were also observed in these species.

Monooxygenation: Oxidative metabolites with *m/z* 16 Da higher than the parent.

Hydroxylation: Oxidative metabolites with a known hydroxyl group

Downloaded from dmd.aspetjournals.org at ASPET Journals on April 18, 2024

DMD Fast Forward. Published on April 2, 2010 as DOI: 10.1124/dmd.110.032755
This article has not been copyedited and formatted. The final version may differ from this version.

DMD Fast Forward. Published on April 2, 2010 as DOI: 10.1124/dmd.110.032755
This article has not been copyedited and formatted. The final version may differ from this version.

Figure 1.

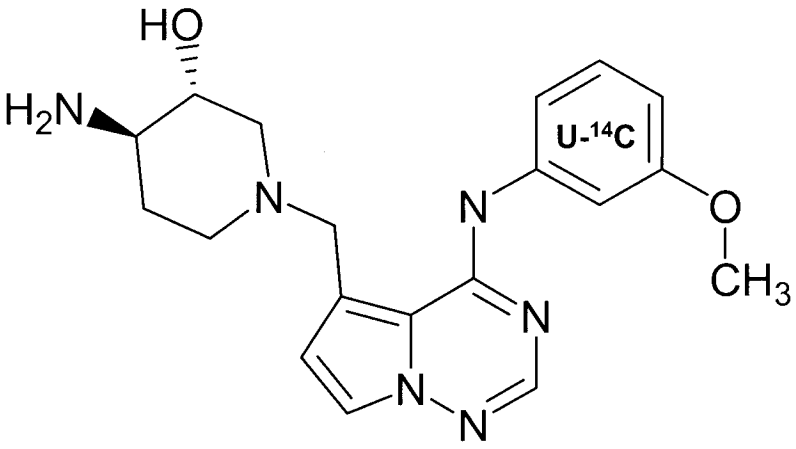

Downloaded from dmd.aspetjournals.org at ASPET Journals on April 18, 2024

DMD Fast Forward. Published on April 2, 2010 as DOI: 10.1124/dmd.110.032755
This article has not been copyedited and formatted. The final version may differ from this version.

Figure 2.

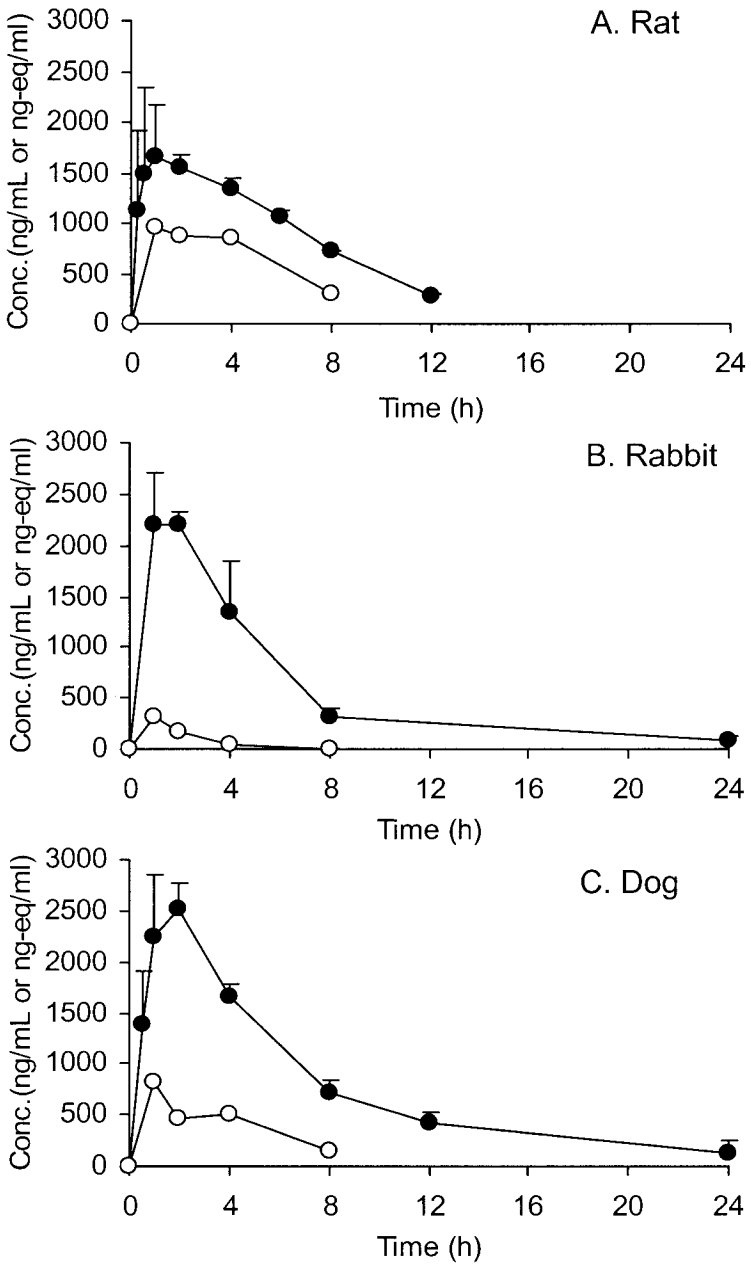

D. AUC (0-8h) for BMS-690514 and total radioactivity (TRA) in rats, dogs and rabbits

	$AUC\ (0\text{-}8h)_{TRA}$ (ng-h/ml)	$AUC\ (0\text{-}8h)_{BMS\text{-}690514}$ (ng-h/ml)	$\%AUC\ (0\text{-}8h)_{BMS\text{-}690514}/AUC\ (0\text{-}8h)_{TRA}$
Rat	9456	5420	57
Rabbit	10,167	709	7
Dog	12,389	3340	27

Downloaded from dmd.aspetjournals.org at ASPET Journals on April 18, 2024

DMD Fast Forward. Published on April 2, 2010 as DOI: 10.1124/dmd.110.032755
This article has not been copyedited and formatted. The final version may differ from this version.

Figure 3.

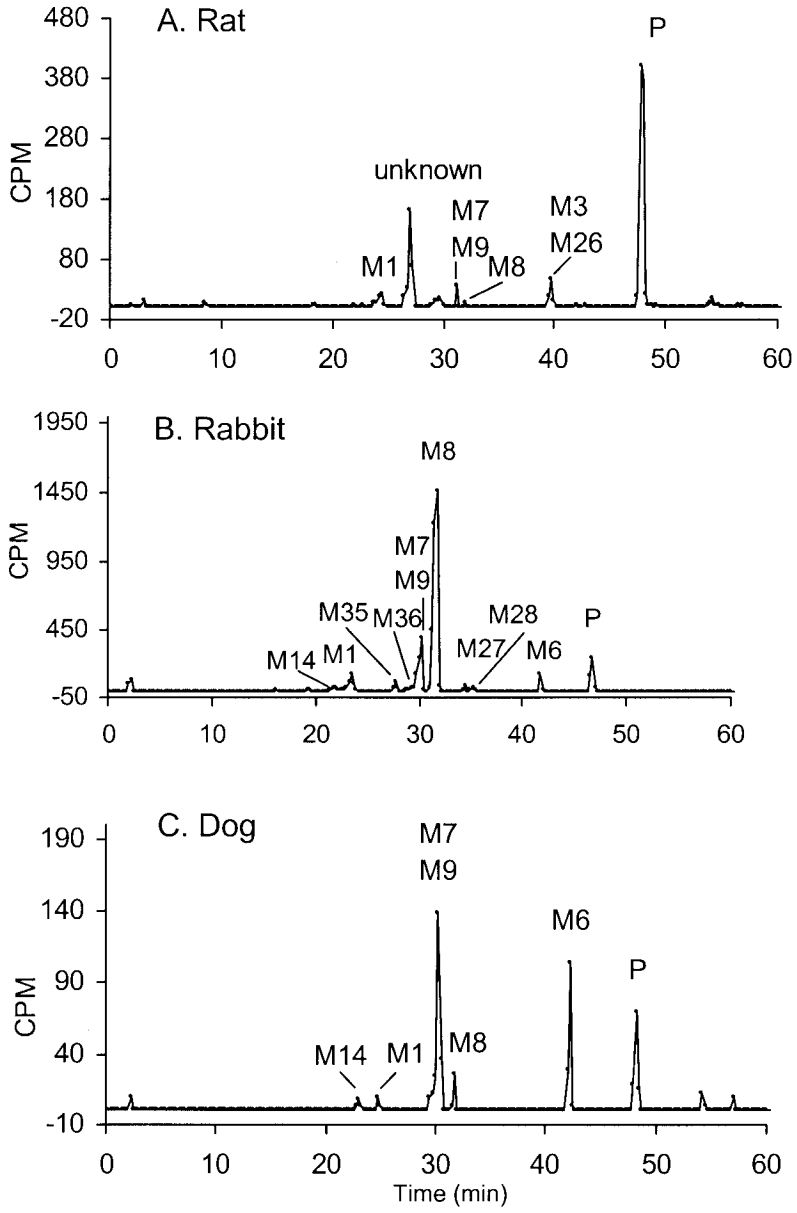

Downloaded from dmd.aspetjournals.org at ASPET Journals on April 18, 2024

DMD Fast Forward. Published on April 2, 2010 as DOI: 10.1124/dmd.110.032755
This article has not been copyedited and formatted. The final version may differ from this version.

Figure 4.

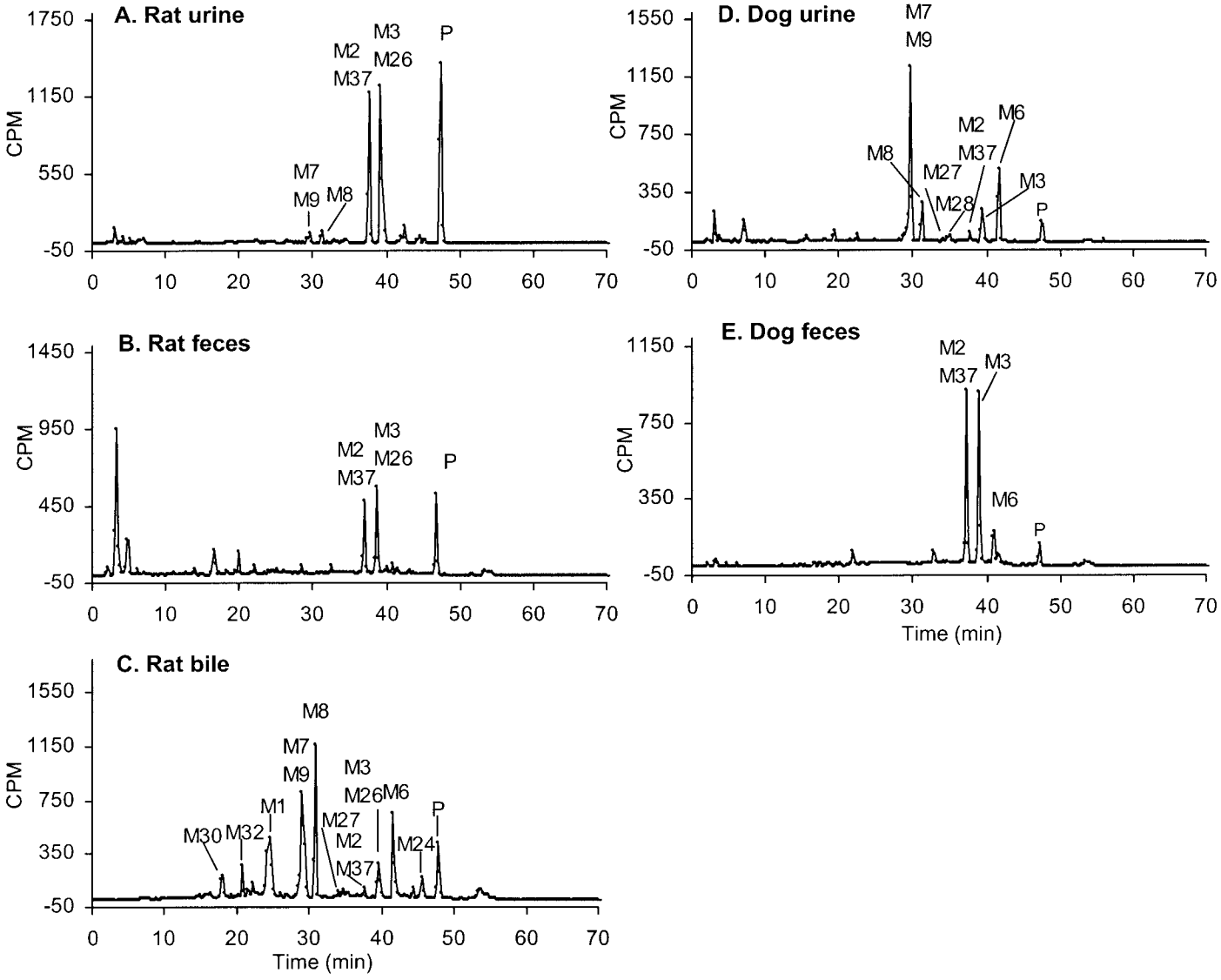

Downloaded from dmd.aspetjournals.org at ASPET Journals on April 18, 2024

Downloaded from dmd.aspetjournals.org at ASPET Journals on April 18, 2024

DMD Fast Forward. Published on April 2, 2010 as DOI: 10.1124/dmd.110.032755
This article has not been copyedited and formatted. The final version may differ from this version.

Figure 5

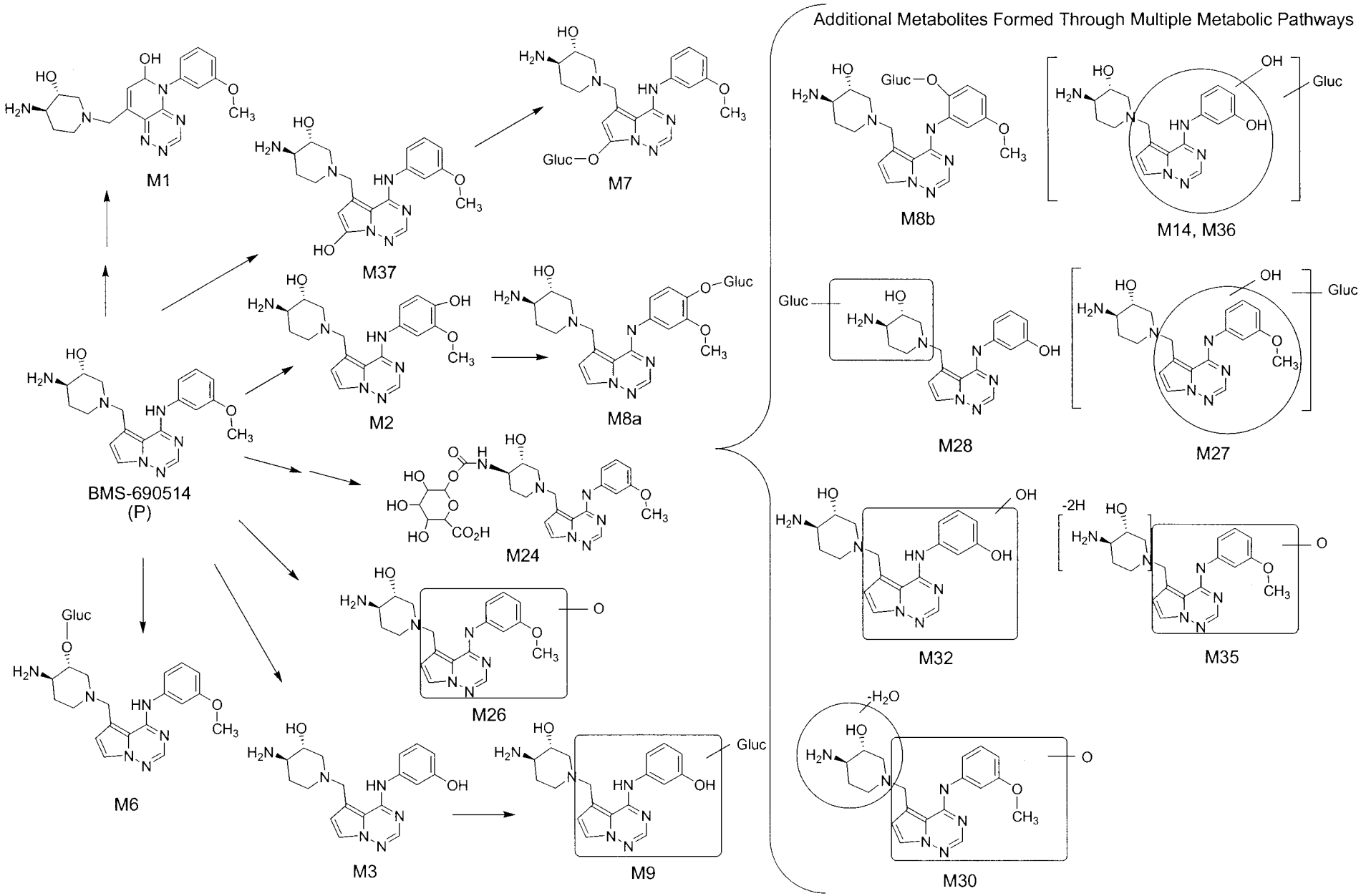

DMD Fast Forward. Published on April 2, 2010 as DOI: 10.1124/dmd.110.032755
This article has not been copyedited and formatted. The final version may differ from this version.

Figure 6

A)

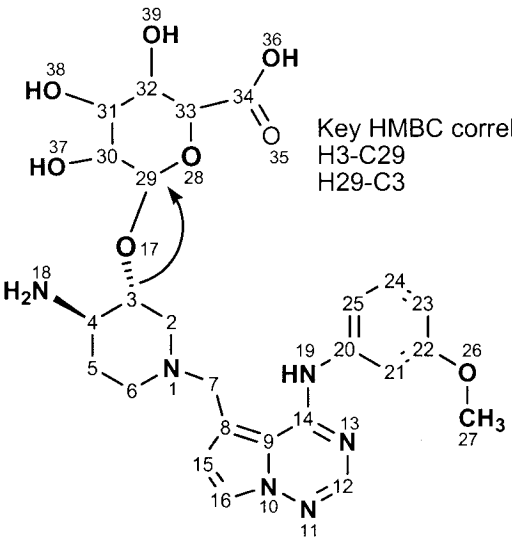

M6

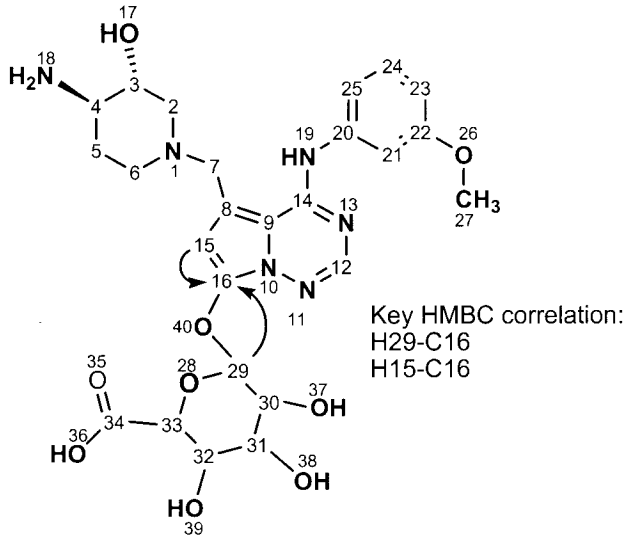

M7

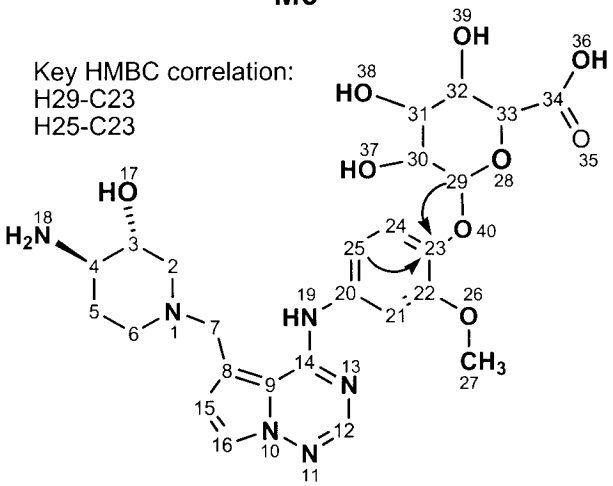

M8a

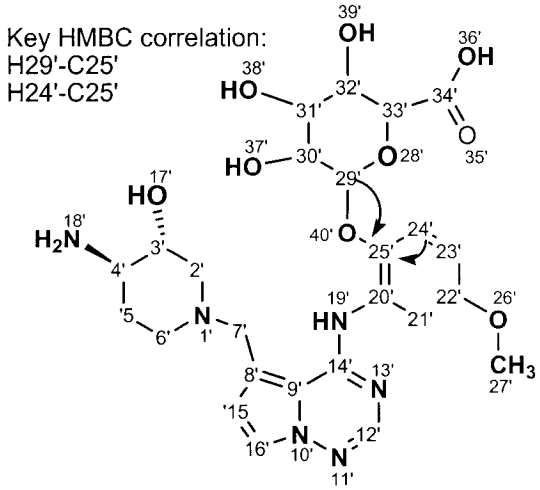

M8b

B) Key NMR chemical shift data of BMS-690514 and metabolites M6, M7, M8a and M8b

Chemical shift (ppm)	BMS-690514	M6	M7	M8a	M8b
H3	3.25	3.79	3.61	3.48	3.48
H4	2.42	3.10	2.96	2.92	3.00
H15	6.57	6.61	6.25	6.57	6.57
H16	7.46	7.48	NA	7.45	7.46
H23	6.73	6.76	6.74	NA	6.87
H25	7.09	6.98	7.00	7.19	NA
C2	58.2	54.6	58.1	58.1	58.1
C3	73.2	74.6	68.2	68.5	68.5
C4	55.0	52.7	55.0	55.1	54.5
C5	31.9	27.6	27.8	28.0	28.0
C15	113.4	113.3	97.7	113.4	113.4
C16	118.4	118.3	140.2	118.7	118.7
C23	110.7	110.6	110.8	146.6	116.1
C25	115.7	115.5	115.5	120.3	143.9

NA = not applicable

Downloaded from dmd.aspetjournals.org at ASPET Journals on April 18, 2024

DMD Fast Forward. Published on April 2, 2010 as DOI: 10.1124/dmd.110.032755
This article has not been copyedited and formatted. The final version may differ from this version.

Figure 7

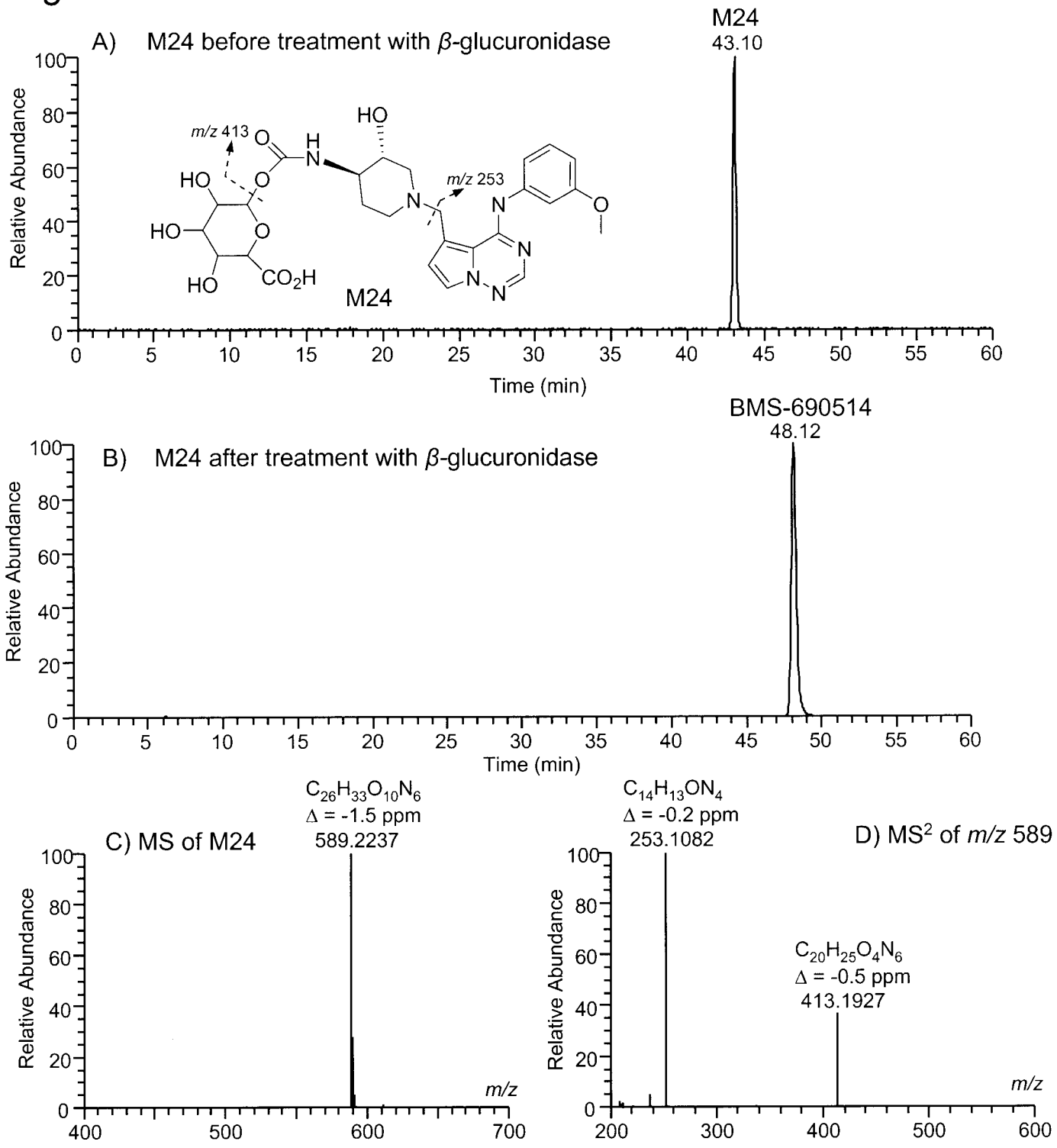

Downloaded from dmd.aspetjournals.org at ASPET Journals on April 18, 2024